



**HAL**  
open science

# Activation of N–O $\sigma$ Bonds with Transition Metals: A Versatile Platform for Organic Synthesis and C–N Bonds Formation

Uroš Todorović, R. Martin Romero, Lucile Anthore-Dalion

► **To cite this version:**

Uroš Todorović, R. Martin Romero, Lucile Anthore-Dalion. Activation of N–O  $\sigma$  Bonds with Transition Metals: A Versatile Platform for Organic Synthesis and C–N Bonds Formation. *European Journal of Organic Chemistry*, 2023, 26 (31), 10.1002/ejoc.202300391 . hal-04235690

**HAL Id: hal-04235690**

**<https://hal.science/hal-04235690>**

Submitted on 10 Oct 2023

**HAL** is a multi-disciplinary open access archive for the deposit and dissemination of scientific research documents, whether they are published or not. The documents may come from teaching and research institutions in France or abroad, or from public or private research centers.

L'archive ouverte pluridisciplinaire **HAL**, est destinée au dépôt et à la diffusion de documents scientifiques de niveau recherche, publiés ou non, émanant des établissements d'enseignement et de recherche français ou étrangers, des laboratoires publics ou privés.



Distributed under a Creative Commons Attribution - NonCommercial - ShareAlike 4.0 International License

# Activation of N–O $\sigma$ Bonds with Transition Metals: A Versatile Platform for Organic Synthesis and C–N Bonds Formation

Uroš Todorović,<sup>[a]†</sup> R. Martin Romero,<sup>[a]†</sup> and Lucile Anthore-Dalion<sup>\*[a]</sup>

**Abstract:** N–O  $\sigma$  bonds containing compounds are versatile substrates for organic synthesis under transition metal catalysis. Their ability to react through both polar (oxidative addition, formation of metallanitrene, nucleophilic substitution) and radical pathways (single electron transfer, homolytic bond scission) have triggered the development of various synthetic methodologies, particularly toward synthesizing nitrogen-containing compounds. In this review, we discuss the different modes of activation of N–O bonds in the presence of transition metal catalysts, emphasizing the experimental and computational mechanistic proofs in the literature to help to design new synthetic pathways toward the synthesis of C–N bonds.

## 1. Introduction

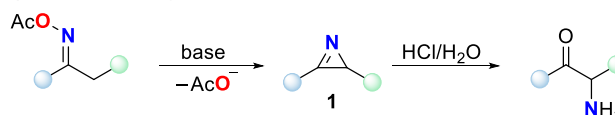
The formation of C–N bonds is central in fine chemistry and is estimated to correspond to 35 % of all reactions in pharmaceutical industries. Traditional methods rely on nucleophilic sources of nitrogen and include the *N*-alkylation of alkyl halides, the reductive amination of carbonyl derivatives, and the cross-coupling of aryl halides with amines.<sup>[1]</sup> In line with the renaissance of radical chemistry, the active development of photoredox pathways, and the emergence of electrophilic aminations, the reactivity of N–O  $\sigma$  bonds (hydroxylamine derivatives, substituted oximes...) has garnered increased interest in the elaboration of complex Nitrogen-containing molecules. The high reactivity of these bonds relies on the electrophilic nitrogen atom, a weak N–O bond, and their propensity to be reduced.

The electrophilic character of *O*-tosyl ketoximes has been recognized since the 1920s when Neber and Friedolsheim used it for synthesizing  $\alpha$ -amino ketones.<sup>[2]</sup> The Neber rearrangement of *O*-acyl ketoximes corresponds to their base-induced rearrangement into  $\alpha$ -amino ketones. After deprotonation of the  $\alpha$ -position, the release of the carboxylate occurs either via an internal  $S_N2$  reaction or a nitrene intermediate and gives 2*H*-azirine **1**, which is then hydrolyzed (Scheme 1a). Based on the same principle, other reactions using electrophilic nitrogen have been designed, i.e., electrophilic aminations.<sup>[3]</sup> In most cases, the nitrogen atom is the electrophilic center, except in particular substrates such as *N*-substituted oxaziridines, where the oxygen atom carries the positive partial charge.<sup>[4]</sup> These substrates are nevertheless out of the scope of the present review.

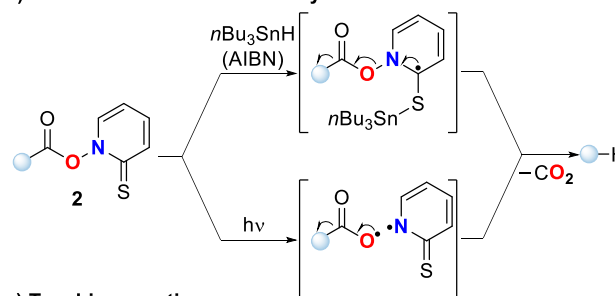
The low bond dissociation energy (BDE) of N–O  $\sigma$  bonds results from the repulsion of the lone electron pairs on the nitrogen and oxygen atoms. This low BDE imparts hydroxylamine derivatives a reactivity similar to chloramines (BDE $\approx$ 63.0 kcal/mol<sup>–1</sup> for the parent hydroxylamine H<sub>2</sub>N–OH vs. 60.5 kcal/mol<sup>–1</sup> for chloramine H<sub>2</sub>N–Cl).<sup>[5]</sup> Hydroxylamine derivatives are, at the same time, less toxic and, in most cases, more stable. The resulting high reactivity of N–O  $\sigma$  bonds compared to other N–Y bonds (e.g., H<sub>2</sub>N–CH<sub>3</sub> BDE= 85.1  $\pm$  0.5 kcal/mol)<sup>[5]</sup> thus allows designing orthogonal reaction processes, which lead to high selectivity in complex molecules. Homolytic fragmentation of an N–O  $\sigma$  bond is, for instance, key to the Barton-Motherwell decarboxylation where a thiohydroxamate ester **2** is reduced under thermal or photoactivation (Scheme 1b).<sup>[6]</sup> Tsuchiya employed the same

strategy with benzophenone oxime esters **3**, where the homolytic cleavage of the N–O bond occurred through photolysis, followed by the decarboxylation of the carboxyl radical. The resulting carbon-centered radical was then trapped by benzene, which created a C–C bond (Scheme 1c).<sup>[7]</sup> These seminal examples demonstrate the high reactivity and high versatility of the N–O  $\sigma$  bond, which can be activated via both polar and radical pathways.

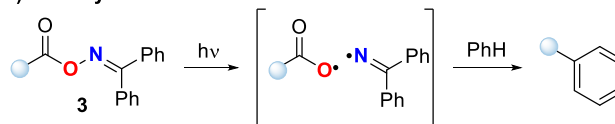
### a) Neber rearrangement



### b) Barton-Motherwell decarboxylation



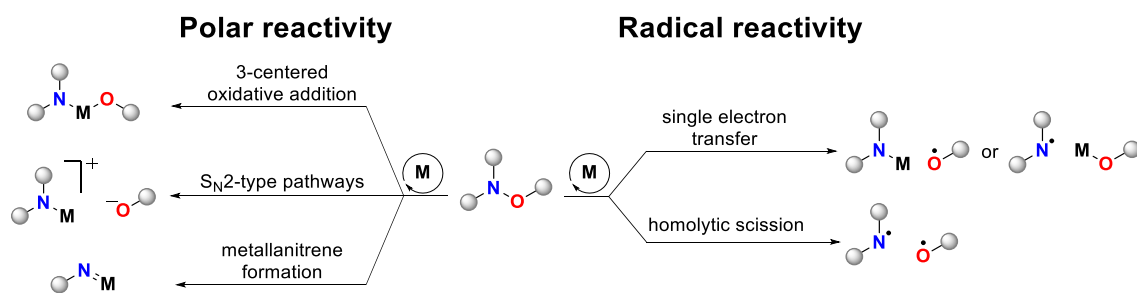
### c) Tsuchiya reaction



Scheme 1. Seminal reactions making use of the high reactivity of N–O  $\sigma$  bonds: a) Neber rearrangement with acyl oximes; b) Barton-Motherwell decarboxylation through thiohydroxamate esters; c) Tsuchiya reaction of benzophenone oxime ester.

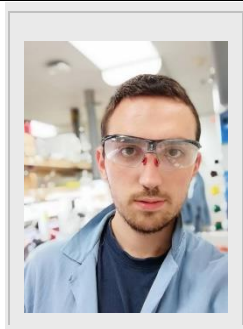
In the presence of transition metals, hydroxylamine derivatives display the same dichotomy, i.e., both polar and radical pathways can be involved. In the case of polar reactivity, one can distinguish three main mechanisms: the classical 3-centered oxidative addition,  $S_N2$ -type pathways, and the formation of metallanitrene intermediates. Radical pathways lead to the generation of nitrogen and/or oxygen radicals via either single electron transfer (SET) or homolytic scission (Scheme 2). The boundaries between the different reaction mechanisms are often difficult to identify, and thus the outcome of the reaction is difficult to predict. A deep understanding of how the fine-tuning of the substrate and the reaction conditions will trigger one or the other pathway could allow one to foresee the outcome, and only some examples of direct proofs are reported in the literature.

While not exhaustively listing the abundant literature about hydroxylamine derivatives' activation with transition metals, this article reviews the different parameters that guide the reactivity of these versatile compounds, especially in their use toward the elaboration of C–N bonds. In particular, we will discuss experimental and computational mechanistic proofs that hint at one or another pathway.

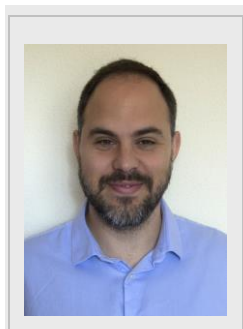


Scheme 2. Polar and radical pathways observed with hydroxylamine derivatives in the presence of transition-metal catalysts M.

Uroš Todorović obtained his BSc at the University of Belgrade and his MSc degree at the University of Paris-Saclay, where he is currently a doctoral student at the LCMCE group. He was always passionate about organic chemistry, and his main areas of interest include methodology development, specifically novel ways of building complexity from simple molecules, as well as the utilization of computational methods in organic chemistry.



Dr. R. Martín Romero received his MSc at the University of Málaga, Spain, in 2012 and obtained his Ph.D. degree at the Institute of Chemical Research of Catalonia (ICIQ) under the supervision of Prof. Kilian Muñiz in 2017, working on hypervalent iodine catalyzed difunctionalization of alkenes. He then joined the group of Dr. Marc Taillefer on an Oril Industries (Servier group) project. In 2019 he moved to the group of Dr. Thibault Cantat, working on formate chemistry and N–O bond activation. In 2022 he joined the group of Prof. Mariola Tortosa as a Maria Zambrano research fellow to develop new C–N bond cleavages.



After obtaining an MSc from ETH Zürich and a diploma from the École Polytechnique, Dr. Lucile Anthore-Dalton received her Ph.D. degree under the supervision of Prof. Samir Zard in 2016, working on xanthate radical chemistry. She then joined the group of Prof. Knochel as a Humboldt research fellow to develop new halogen-lanthanides exchanges. In 2019, she was recruited as CNRS Researcher. Her research interests include the catalytic activation of oxygenated compounds (N-oxides, esters), developing new catalytic synthetic methodologies, and the corresponding mechanistic investigations.



## 2. Oxidative addition of the N–O $\sigma$ bond to transition metal

According to the scientific consensus,<sup>[8]</sup> the oxidative addition of hydroxylamine derivatives corresponds to the addition of the N–O bond to a low-valent metal center [M] to form two new bonds, [M]–N and [M]–O, with an increase of +2 in the redox state of the metal center. The first experimental proof for an oxidative addition of an N–O bond to a metal complex was described by Deeming et al. in 1990. The trinuclear osmium cluster  $[\text{Os}_3(\text{CO})_{10}(\text{MeCN})_2]$  (**4**) reacted with acetone oxime (**5**), initially providing an oxidative addition of the O–H bond and leading to the hydrido complex  $[\text{Os}_3(\mu\text{-H})(\mu\text{-Me}_2\text{C=NO})(\text{CO})_{10}]$ . Upon reflux in octane for 2 h, the osmium cluster isomerized into the non-hydrido cluster  $[\text{Os}_3(\mu\text{-OH})(\mu\text{-Me}_2\text{C=N})(\text{CO})_{10}]$  (**6**). Complex **6** was obtained in overall yield of 22 % over two steps, and its structure has been confirmed by X-ray crystallography. The authors suggested that the hydroxy compound **6** resulting from the oxidative addition of the N–O bond was thus the thermodynamic product (Scheme 3a).<sup>[9]</sup>

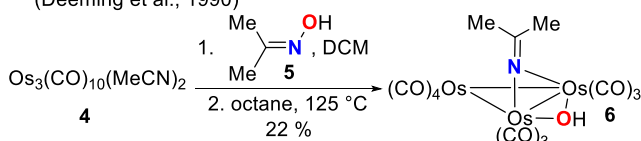
A direct oxidative addition of an N–O bond was also reported in the reaction between acetone oxime (**5**) and *trans*-[ReCl(N<sub>2</sub>)(dppe)<sub>2</sub>] (**7**) (dppe=1,2-bis(diphenylphosphino)ethane) in the presence of Ti[H<sub>2</sub>SO<sub>4</sub>] as chlorine abstractor. The resulting *trans*-[Re(OH)(N=CMe<sub>2</sub>)(dppe)<sub>2</sub>] (**8**) was characterized by X-ray crystallography. The electron-rich rhenium metal center was believed to favor the oxidative addition of the N–O versus the O–H bond. Its  $\pi$ -donor character, combined with the steric hindrance induced by the bulky diphosphine ligands, helped to stabilize the final complex, which bears a  $\pi$ -acceptor linear ligand N=CMe<sub>2</sub>. The  $\pi$ -backbonding promoted the formation of a significant double-bond character, i.e., an azavinylidene complex, between the rhenium core and the nitrogen atom. The short Re–N distance in the X-ray structure proved the double-bond character (1.901 Å, shorter than the Re–N average value of 2.107 Å, Scheme 3b).<sup>[10]</sup>

Rosenthal, Tillack et al. disclosed in the late 90s examples of N–O bonds oxidative addition to group IV metal complexes. They showed by X-ray crystallography that the zirconocene complex  $[\text{Cp}_2\text{Zr}(\text{Pyr})(\text{Me}_3\text{SiC}_2\text{SiMe}_3)]$  (Pyr = pyridine, **9**) led to the dimer **10** in the presence of 1,2-benzisoxazole. The Zr–O and Zr–N bonds were formed upon opening the 5-membered ring (Scheme 3c).<sup>[11]</sup> To avoid the competitive oxidative addition of the O–H bond of oximes, silylated oximes **11** were reacted with titanocene  $[\text{Cp}_2\text{Ti}(\text{Me}_3\text{SiC}_2\text{SiMe}_3)]$  (**12**). Intermediate coordination of the nitrogen and oxygen atoms to the metal core was assumed to trigger the N–O bond scission. X-ray analysis confirmed the formation of titanocene complex  $[\text{Cp}_2\text{Ti}(\text{N=CR}_2)(\text{OSiMe}_3)]$  (**13**). The Ti–N bond length showed a single bond character (1.903 Å, Scheme 3d).<sup>[12]</sup>

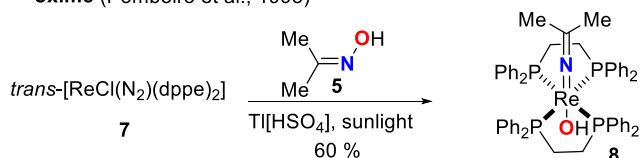
More recently, the same reactivity has been demonstrated with late transition metals. Ohe, Okamoto et al. were able to synthesize ruthenium(IV) ketimido complexes **14** resulting from the oxidative addition of oxime ester **15** to  $[\text{RuX}_2(\text{PPh}_3)_3]$  (X=Cl or

Br). As in the case of Pombeiro's rhenium complex **8**,<sup>[10]</sup> the short bond distance (1.790 Å) was proof of a significant double bond character, which was supported by natural bond orbital (NBO) analysis (Scheme 3e).<sup>[13]</sup> Love et al. isolated the Ni(II) complex **16** resulting from the oxidative addition of the N–O bond of *N*-adamantyl oxaziridine **17** to [(dtbpe)Ni(0)] complex (dtbpe = 1,2-bis(di-*tert*-butylphosphino)ethane). This complex proved stable enough at –30 °C to grow crystals (Scheme 3f) but decomposed at higher temperatures.<sup>[14]</sup> Morandi et al. recently demonstrated the ability of the nickel(0) complex [(dcype)Ni] (dcype = 1,2-bis(dicyclohexylphosphino)ethane) to insert in the N–O bond of benzoxazole **18**. X-ray, NMR, and HRMS analyses confirmed the structure of the resulting Ni(II) complex **19** (Scheme 3g).<sup>[15]</sup>

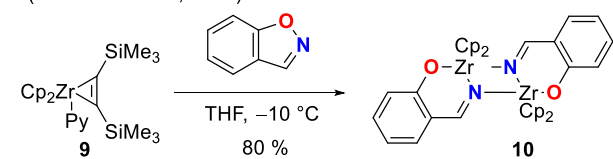
**a) Reaction of acetone oxime and an Os(0) complex**  
(Deeming et al., 1990)



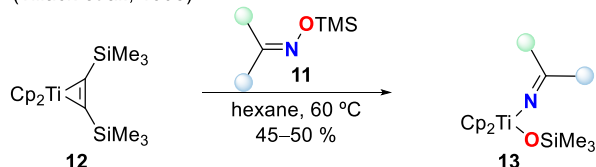
**b) Formation of an azavinylidene Re-complex from O-acetyl oxime**  
(Pombeiro et al., 1998)



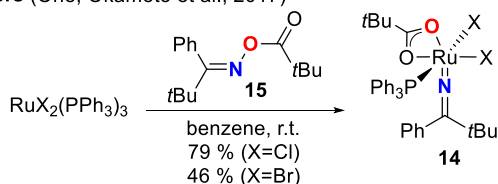
**c) N–O bond cleavage with a zirconocene complex**  
(Rosenthal et al., 1996)



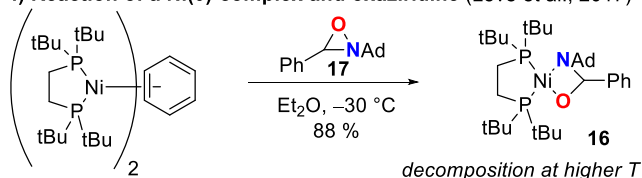
**d) N–O bond cleavage with a titanocene complex**  
(Tillack et al., 1998)



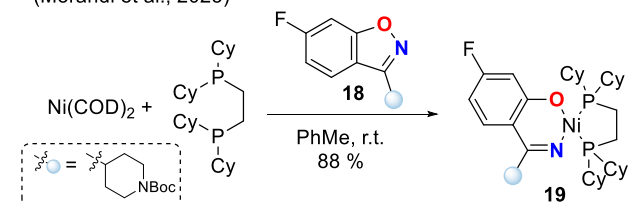
**e) Ruthenium(IV) ketimido complexes obtained from oxime esters**  
(Ohe, Okamoto et al., 2017)



**f) Reaction of a Ni(0)-complex and oxaziridine** (Love et al., 2017)



**g) Reaction of a Ni(0)-complex and benzoxazole**  
(Morandi et al., 2023)



Scheme 3. Selected examples of complexes obtained by insertion of transition metal complexes in N–O bonds of various *N*-oxides whose structures were confirmed by X-ray analysis. Cp = cyclopentadienyl; dppe = 1,2-bis(diphenylphosphino)ethane; Cy = cyclohexyl; COD = 1,5-cyclooctadiene.

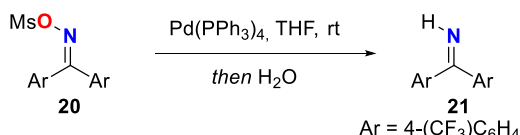
These selected examples evidence the possibility to activate N–O bonds with transition metals via oxidative addition. Based on these seminal examples, the ability of hydroxylamine derivatives to undergo oxidative addition to transition metals was utilized to develop metal-catalyzed C–N bond formations.

However, X-ray structures are not giving any information on the mechanistic pathway followed, and more investigations are required to distinguish between the classical 3-centered oxidative addition,  $\text{S}_{\text{N}}2$ -type mechanistic pathways, and radical pathways. Intensive work has been done to differentiate between those pathways, particularly in palladium- and copper-catalyzed reactions, which will be discussed below.

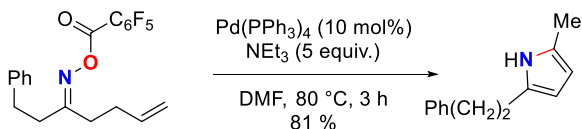
## 2.1. Pd-catalyzed reactions

In the late 90s, Narasaka et al. made an interesting observation in the reaction of *O*-sulfonyl oxime derivative **20** with  $\text{Pd}(\text{PPh}_3)_4$ . The derived imine **21** was observed after hydrolysis, hinting at an oxidative addition of the N–O bond to the Pd(0) and a putative Pd(II) intermediate (Scheme 4a). Using this hypothesis, Pd-catalyzed aza-Heck reactions of *O*-acyl oximes bearing a pendant alkene group were developed, leading to pyrroles (Scheme 4b). The authors found that using a pentafluorobenzoyl group as *O*-substituent completely suppressed the undesirable Beckmann rearrangement of the oxime.<sup>[16]</sup> Based on the same mechanistic rationale, the group developed Pd-catalyzed syntheses of *N*-heterocycles<sup>[17]</sup> such as pyrroles,<sup>[16,18]</sup> spiro imines,<sup>[19]</sup> 1-azaazulenes,<sup>[20]</sup> pyridines,<sup>[21]</sup> imidazoles,<sup>[22]</sup> isoindoles,<sup>[23]</sup> isoquinolines,<sup>[21,24]</sup> or phenanthridines (Scheme 4c).<sup>[24]</sup> A similar oxidative addition may be involved in the cyclobutanone *O*-benzoyl oxime Pd-catalyzed ring cleavage (Scheme 4d).<sup>[25]</sup> Fürstner et al. finally demonstrated the applicability of this methodology in the total synthesis of butylcycloheptylprodigiosin (**22**) (Scheme 4e).<sup>[26]</sup>

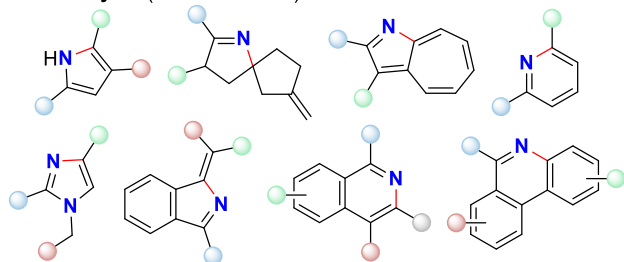
**a) Reaction of an *O*-methylsulfonyl oxime in presence of a Pd(0)-complex (Narasaka et al., 1999)**



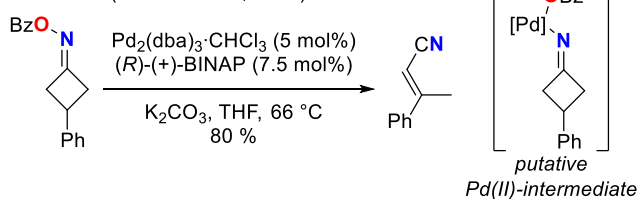
**b) Pd-catalyzed aza-Heck reaction of *O*-acyl oximes (Narasaka et al., 1999)**



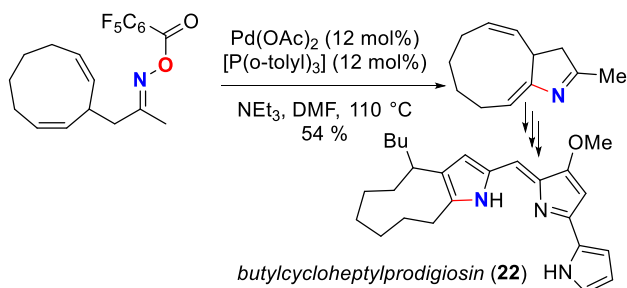
**c) Accessible heterocycles from *O*-substituted oximes via Pd-catalysis (Narasaka et al.)**



**d) Pd(0)-catalyzed ring opening of cyclobutanone *O*-benzoyl oximes (Uemura et al., 2000)**



**e) Application of the Pd-catalyzed reaction of oxime esters in total synthesis (Fürstner et al., 2005)**

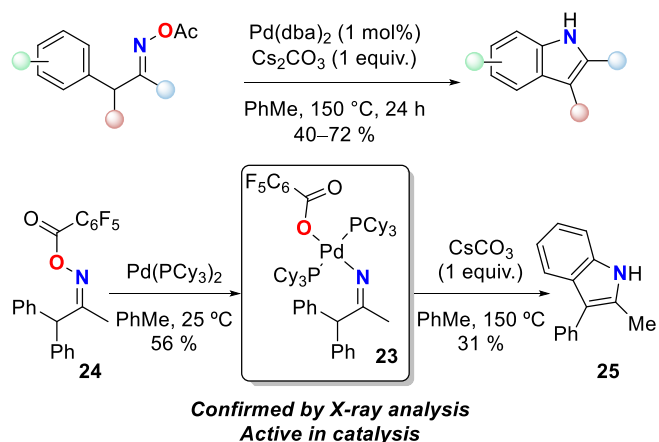


Scheme 4. Reactions based on a possible oxidative addition of N–O bond to a [Pd] species: a) Preliminary results of Narasaka et al. when reacting a Pd(0)-complex and an oxime; b) Pd-catalyzed aza-Heck reaction; c) Accessible *N*-heterocycles via the same mechanistic rationale; d) Pd-catalyzed ring-opening of cyclobutanone oxime ester by Uemura et al.; e) Application to the synthesis of butylcycloheptylprodigiosin (**22**) by Fürstner et al.

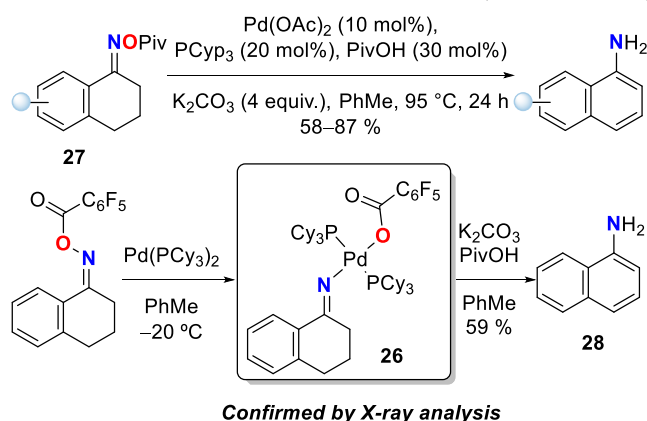
The actual oxidative addition of an N–O bond to a Pd(0) species was only proven in 2010 when Hartwig et al. isolated the Pd(II)-complex intermediate **23**, resulting from the oxidative addition of  $[\text{Pd}(\text{PCy}_3)_2]$  in the *O*-pentafluorobenzoyl oxime **24**. The authors confirmed that the isolated Pd(II)-complex **23** led to the same product as their catalytic methodology, namely the indole product **25**, and was active in catalysis (Scheme 5a).<sup>[27]</sup> The same strategy was employed later by Stahl, who isolated Pd(II)-complex **26** when developing a Pd-catalyzed 1-aminonaphthalene synthesis from the corresponding tetralone pivaloyl oximes **27**. The authors also confirmed that complex **26** led to the corresponding 1-aminonaphthalene **28** (Scheme 5b).<sup>[28]</sup> However, in both cases,

no information was given on the mechanistic pathway. As demonstrated later by Bower et al.,<sup>[29]</sup> the formation of Pd(II)-complexes **23** and **26** should involve single electron transfers since electron-rich phosphine ligands  $\text{PCy}_3$  are used. Section 4.3 (vide infra) will discuss this dichotomous reactivity in more detail.

**a) Pd-catalyzed indole synthesis (Hartwig et al., 2010)**



**b) Pd-catalyzed 1-aminonaphthalene synthesis (Stahl et al., 2013)**



Scheme 5. Experimental proofs for an oxidative addition of N–O bonds to Pd(0) complexes: synthesis of indoles by Hartwig et al. (a), of 1-aminonaphthalene derivatives by Stahl et al. (b), and corresponding isolated complexes.

Inspired by Narasaka's pioneering work,<sup>[18]</sup> Bower et al. developed 5-exo-iminopalladation reactions, leading to the intramolecular elaboration of an N–C(sp<sup>3</sup>) bond.<sup>[30]</sup> In the presence of an extended alkyl chain, the authors synthesized 3,4-dihydro-2*H*-pyrrole **29** bearing an exocyclic alkene (Scheme 6a), whereas Narasaka et al. were obtaining pyrroles (Scheme 4b). A stereoselective reaction was even doable using a chiral TADDOL-derived phosphoramidite ligand.<sup>[30b]</sup>

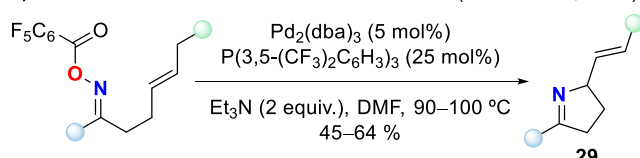
Some aspects are important in these modifications. The electron-deficient phosphine ligand  $\text{P}(3,5\text{-(F}_3\text{C)}_2\text{C}_6\text{H}_3)_3$  may enhance the  $\sigma$ -donation from the imine ligand to the metal after oxidative addition. This  $\sigma$ -donation will increase the N–Pd bond strength and decrease the basicity of the nitrogen lone pair, suppressing the competitive protodepalladation to the NH imine. In addition, lowering the electron density of the Pd(II) species could accelerate the alkene migratory insertion. Indeed, the authors showed that an electron-neutral phosphine like  $\text{PPh}_3$  led to more protodepalladation. In contrast, an electron-rich phosphine such as  $\text{P}(\text{tBu})_3$  promoted the formation of an iminyl radical via N–O bond homolysis (see section 4.3 for more details).<sup>[29]</sup> The bulky

ligand should finally be crucial for the regioselectivity of the  $\beta$ -hydride elimination, resulting from steric effects.<sup>[30c]</sup>

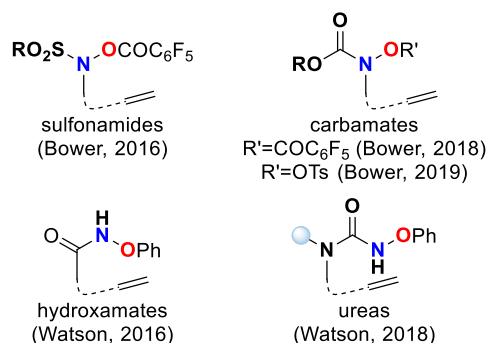
Bower also explained the key effect of the *O*-pentafluorobenzoyl substituent already observed by Narasaka et al.<sup>[16]</sup> After oxidative addition, the decoordination of the benzoate ligand leads to the formation of a cationic Pd(II)<sup>+</sup> intermediate, which promotes an efficient migratory insertion of the alkene. Using the electron-poor pentafluorobenzoate facilitates the decoordination, and its subsequent spontaneous protodecarboxylation under reaction conditions (90 °C, NEt<sub>3</sub> 2 equiv. in DMF) prevents its recoordination.<sup>[30d]</sup>

Beyond the Narasaka-Heck reaction, other vicinal imino-functionalizations (-acylation,<sup>[30d]</sup> -carboxylation,<sup>[30d]</sup> -arylation,<sup>[30d,31]</sup> -vinylation,<sup>[30d]</sup> -alkynylation,<sup>[30d]</sup> -halogenation<sup>[32]</sup>) have been developed, making use of the migratory insertion of an alkene in the iminopalladium(II) intermediate. Aza-Heck reactions were also designed with other hydroxylamine derivatives (sulfonamides,<sup>[33]</sup> carbamates,<sup>[34]</sup> hydroxamates,<sup>[35]</sup> ureas<sup>[36]</sup>) in the presence of Pd-catalysts, using the same strategy (Scheme 6b). Efficient enantioselective processes have been reported in the case of *N*-(tosyloxy) carbamate derivatives.<sup>[34b]</sup> Albeit no direct proof for an oxidative addition of the N–O bond to the metal catalyst exists, indirect results, such as the inactivity of the corresponding N–H compounds under the reaction conditions or the decarboxylation of the pentafluorobenzoate ligand, hinted at the implication of a similar mechanistic pathway.

**a) Narasaka-Heck reaction with oxime esters** (Bower et al., 2013)



**b) Reactive substrates under similar reaction conditions**



Scheme 6. a) Narasaka-Heck reaction developed by Bower et al. on oxime derivatives; b) Substrates reacting under similar reaction conditions via a supposed similar pathway.

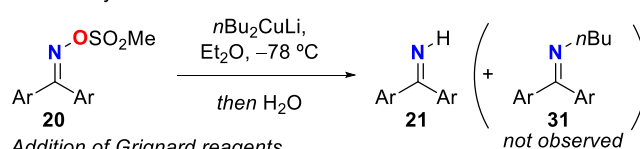
## 2.2. Cu-catalyzed oxidative additions: ambiguous results

The use of copper for N–O bond scission was initially reported by Narasaka et al. in 1997. When reacting the Gilman reagent *n*Bu<sub>2</sub>CuLi with *O*-methylsulfonyl oxime **20**, they observed the formation of the corresponding NH-imine **21** upon hydrolysis. This observation led to the hypothesis that an oxidative addition of the N–O bond to the Cu(I) species, giving a putative Cu(III)-intermediate **30**, would be possible. In Et<sub>2</sub>O, the latter, however, was supposed to be unable to undergo reductive elimination to the desired *N*-butyl imine **31**. Employing an HMPA/Et<sub>2</sub>O (HMPA = hexamethylphosphoramide) mixture as a solvent finally allowed the authors to develop a Cu(I)-catalyzed addition of Grignard reagents to *O*-sulfonyl oxime **20** (Scheme 7a).<sup>[37]</sup>

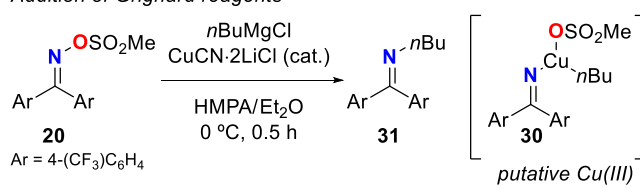
Ten years later, Liebeskind et al. made a similar observation in the Cu-catalyzed *N*-imination of boronic acids or organostannanes with *O*-acyl ketoximes **32**. Upon aqueous work-up, a 1:1 mixture of the catalyst and the starting ketoxime **32** led to the corresponding NH-imine, hinting at an oxidative addition of the N–O bond. Reacting aldoximes under the same conditions leads to nitrile derivatives **33** instead of imine **34**. This result was an additional indirect proof for an oxidative addition pathway (Scheme 7b).<sup>[38]</sup> Indeed, nitrile **33** could arise from a  $\beta$ -hydride elimination from the putative Cu(III)-intermediate. Based on these observations, the same group reported a Cu(I)-mediated cross-coupling of boronic acids and organostannanes with *O*-acetyl hydroxamic acids **35** (Scheme 7c). In this case, a stoichiometric amount of copper was required, which was ascribed to the higher stability of a possible Cu-amido complex. Again, the mechanism is supposed to go through oxidative addition of the *N*-oxide to the Cu(I) species since, in the absence of nucleophiles and after hydrolysis, the primary amide PhCONH<sub>2</sub> was obtained.<sup>[39]</sup> Nevertheless, radical pathways cannot be completely ruled out and will be discussed in section 4.2 (*vide infra*).

**a) Cu(I)-catalyzed addition of Grignard reagents to oximes** (Narasaka et al., 1997)

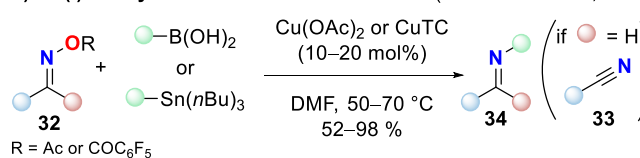
*Preliminary observation*



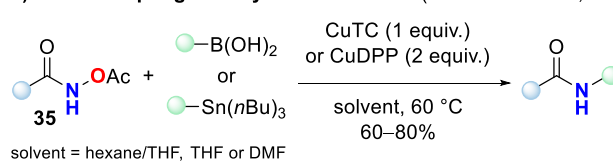
*Addition of Grignard reagents*



**b) Cu(I)-catalyzed *N*-imination with oximes** (Liebeskind et al., 2007)



**c) Cross coupling with hydroxamic acids** (Liebeskind et al., 2008)



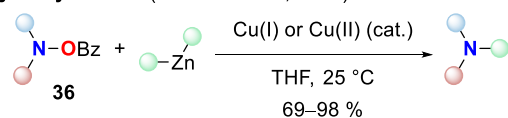
Scheme 7. Examples of Cu-mediated reactions of oxime (a,b) and hydroxamate derivatives (c) supposed to happen through oxidative addition of the N–O bond to copper(I) complexes. HMPA = hexamethylphosphoramide; TC = thiophene-2-carboxylate; DPP = diphenylphosphinate.

In 2004, Johnson et al. reported the Cu-catalyzed electrophilic amination of organozinc reagents with *O*-benzoyl hydroxylamine derivatives **36** (Scheme 8a).<sup>[40]</sup> In a follow-up publication, the group postulated that three different pathways could be involved in this reaction: a classical 3-centered oxidative addition pathway as hypothesized by Narasaka et al., an S<sub>N</sub>2-type mechanism, and a radical pathway (see Scheme 2).

The retention of configuration observed alongside the reaction first ruled out a radical mechanism. The so-called endocyclic

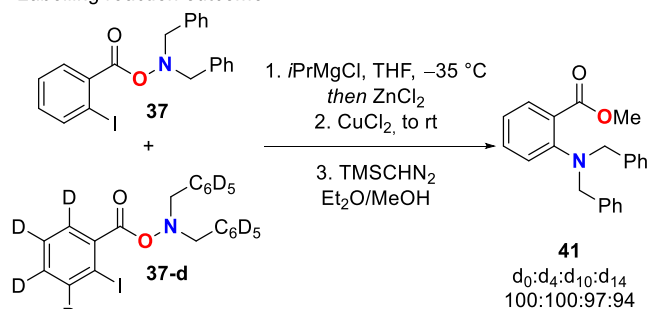
restriction test was performed to distinguish between an  $S_N2$  and an oxidative addition mechanism. Under the reaction conditions, *O*-(2-iodobenzoyl)hydroxylamine **37** was supposed to form Cu(I)-intermediate **38**, resulting from the successive iodine-magnesium, magnesium-zinc, and zinc-copper exchanges. An intramolecular  $S_N2$  reaction is forbidden because of the strained transition state **39**, whereas an intramolecular oxidative addition through transition state **40** is allowed. Thus, if the reaction followed only an intramolecular pathway, it would validate the hypothesis of an oxidative addition mechanism. In the competition reaction between substrate **37** and its D-labelled version **37-d**, the authors observed both non-crossover (**41-d<sub>0</sub>** and **41-d<sub>14</sub>**) and crossover products (**41-d<sub>4</sub>** and **41-d<sub>10</sub>**) in similar amounts ( $d_0:d_4:d_{10}:d_{14}$  100:100:97:94). This outcome could only arise via an intermolecular pathway, therefore an  $S_N2$ -type mechanism and not a 3-centered oxidative addition (Scheme 8b).<sup>[41]</sup>

**a) Cu-catalyzed electrophilic amination with *O*-benzoyl hydroxylamines** (Johnson et al., 2007)

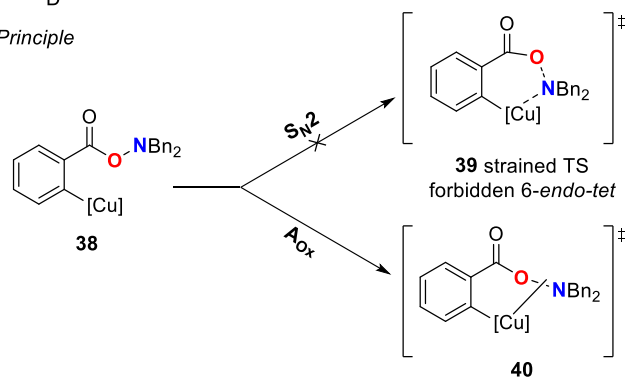


**b) Endocyclic restriction test - Proof for an intermolecular pathway** (Johnson et al., 2007)

Labelling reaction outcome



Principle



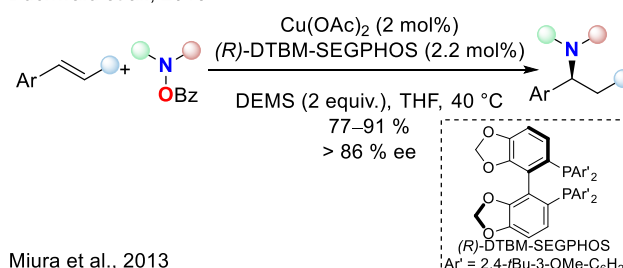
Scheme 8. a) Cu-catalyzed electrophilic amination with diorganozinc reagents; b) Reaction outcome and principle of the endocyclic restriction test performed by Johnson et al.

Tobisch confirmed these findings in 2016 by DFT calculations on a similar electrophilic hydroamination of alkenes<sup>[42]</sup> concomitantly developed by the groups of Miura<sup>[43]</sup> and Buchwald<sup>[44]</sup> in 2013 (Scheme 9a). The reaction involved a copper catalyst which is supposed to react via initial alkene hydrocupration, producing an alkyl copper(I). Tobisch's study validated this assumption. Initially, Buchwald et al. had proposed a classical 3-centered oxidative addition pathway forming a Cu(III)-intermediate.<sup>[44]</sup> The subsequent reductive elimination would finally promote the

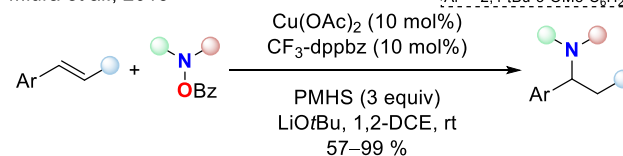
formation of the desired hydroaminated product. According to the computational studies, a pre-coordination of the benzoate on the metallic center occurs before the N–O bond scission, forming intermediate **42**. Among the possible oxidative addition pathways, DFT calculations suggested a favorable  $S_N2$ -reminiscent reactivity on the N core through the nucleophilic attack of the copper center and benzoate dissociation ( $TS_{SN2}$ ,  $\Delta G^\ddagger=12.0$  kcal.mol<sup>-1</sup> from **42**). The alternative classical 3-center oxidative addition of the N–O bond showed a more energetically demanding pathway ( $TS_{OA}$ ,  $\Delta G^\ddagger=23.3$  kcal.mol<sup>-1</sup> from **42**) and, therefore, a less accessible route (Scheme 9b).<sup>[42]</sup> A similar mechanism was proposed based on experimental and computational results for Rh(III)-catalyzed reaction of hydroxamate derivatives with alkynes.<sup>[45]</sup>

**a) Cu-catalyzed hydroamination of styrene derivatives**

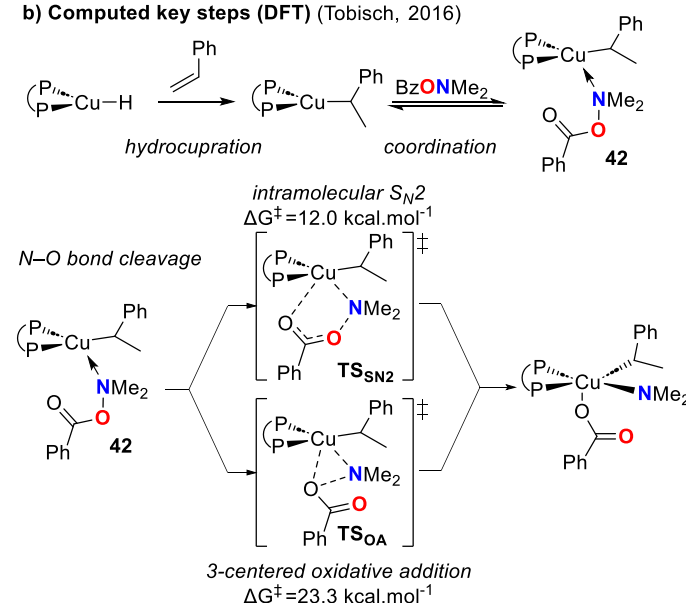
Buchwald et al., 2013



Miura et al., 2013



**b) Computed key steps (DFT)** (Tobisch, 2016)



Scheme 9. a) Reductive Cu-catalyzed hydroamination of styrene derivatives with *O*-benzoyl hydroxylamines described concomitantly by Buchwald et al. and Miura et al.; b) Key steps according to computational results by Tobisch. DEMS = diethoxymethylsilane; PMHS = polymethylhydrosiloxane; dppbz = 1,2-([3,5-(CF<sub>3</sub>)<sub>2</sub>C<sub>6</sub>H<sub>3</sub>]P)<sub>2</sub>C<sub>6</sub>H<sub>4</sub>; 1,2-DCE = 1,2-dichloroethane.

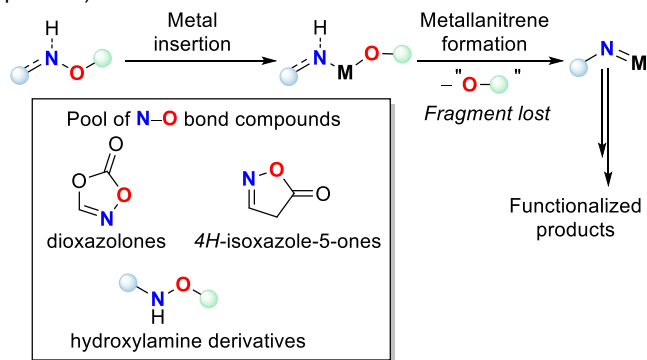
These last examples show the drastic influence of the nature of the *N*-oxide. In the case of oxime derivatives, the classical three-center oxidative addition pathway is favored in the presence of copper(I) catalysts. However, *O*-acylated hydroxylamines are more prone to reacting through an  $S_N2$ -type oxidative addition under similar reaction conditions.



Surprisingly, mechanistic proofs for a catalytic pathway going through oxidative addition of *N*-oxide derivatives to metallic species are rare. Yet, the large variety of isolated metal-complexes resulting from oxidative addition with Os-, Re-, Zr-, Ti-, Ru-, Ni-, or Pd-complexes (see Scheme 3 and Scheme 5) demonstrates the high reactivity of N–O bond containing compounds toward transition metal complexes and should allow the design of new catalytic reactions.

### 3. Metallanitrenes formation from N–O $\sigma$ bonds

As discussed in Section 2, various metals can oxidatively insert into the N–O bond. Under certain conditions, the oxygenated ligand is lost, and intermediate metallanitrene species can be obtained, which can then engage in further reactivity. This nitrene pathway is favored when the oxygenated part can undergo decarboxylation (i.e., with *4H*-isoxazole-5-ones or with dioxazolones<sup>[46]</sup>), or when the oxygenated part is a poor ligand (i.e., because of steric bulkiness, Scheme 10). In the latter case, the remaining oxygen-containing part of the molecule can be incorporated into the final product (i.e., in an amino-oxygenation process).



Scheme 10. Principle of metallanitrene generation from N–O bond-containing compounds and examples of substrates leading preferentially to metallanitrenes.

Although nitrenes are highly reactive species, which can be considered nitrogen analogs of carbenes,<sup>[47]</sup> they are only formed and observed as intermediates.<sup>[48]</sup> Classically, nitrenes can be prepared as transient intermediates from azides via the release of dinitrogen. The fact that a non-stabilized nitrene can insert into a C–H bond to perform an amination reaction speaks to the synthetic utility of this intermediate.<sup>[49]</sup> However, due to this extreme reactivity, a need for better selectivity and reaction control arises. Nitrenes can be stabilized either with silylenes<sup>[50]</sup> or by reducing transition metals, the latter being the most popular method. It should be noted that the description of metallanitrene species is somewhat inconsistent throughout the literature, as both Schrock- and Fischer-type species might explain the observed reactivity. Moreover, these complexes are mostly redox active at the nitrogen atom, and radical pathways can often explain their reactivities. Therefore, it is essential to be aware of the nature of this species, which is highly dependent on the involved metal, ligands, and *N*-derivatives.<sup>[51]</sup> This approach paves the way toward reactivity tuning, as choosing the metal center and coordinated ligands can influence the nature and the reactivity of the resulting stabilized nitrene.<sup>[52]</sup>

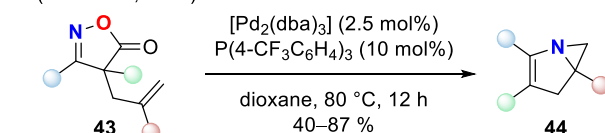
### 3.1 Decarboxylative transformations

Various classes of heterocycles, such as differently substituted dioxazolones and isoxazole derivatives containing the N–O bond, can lead to nitrene species upon decarboxylation of the substrate (Scheme 10). This process unlocks synthetic access points to heterocyclic structures which can't be otherwise easily prepared and enable interesting ring rearrangements.

Ohe et al. showed that it is possible to convert *4H*-isoxazol-5-ones bearing a pendant alkene **43** into 1-azabicyclo[3.1.0]hex-2-enes **44** (Scheme 11a).<sup>[53]</sup> These substrates are easily obtained from the corresponding  $\beta$ -ketoester. Fang et al. then investigated the reaction mechanism by utilizing DFT calculations, and their findings were close to the initial assumption by Ohe's research team. The main mechanistic steps include the formation of the oxidative adduct **45**, which undergoes decarboxylation to the palladium-stabilized vinyl nitrene **46**. According to computational studies, olefin coordination further stabilizes this metallanitrene intermediate. Then, olefin insertion takes place to form the palladacycle **47**. This step is followed by reductive elimination to regenerate the Pd(0)-catalyst, giving the bicyclic system **44** (Scheme 11b).<sup>[54]</sup>

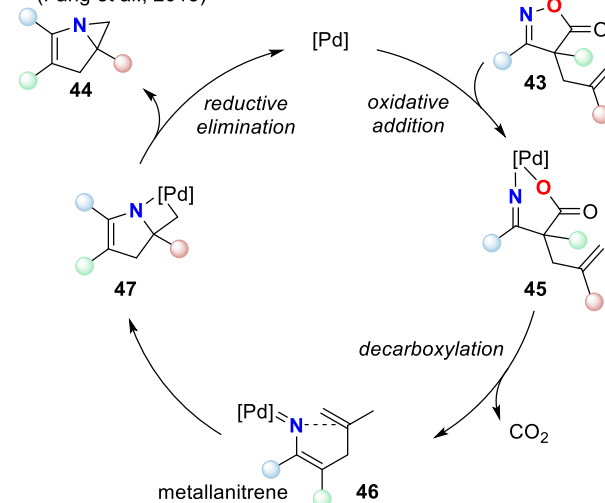
#### a) Pd-catalyzed aziridination from *4H*-isoxazole-5-ones

(Ohe et al., 2011)



#### b) Mechanistic proposal based on computational studies

(Fang et al., 2013)



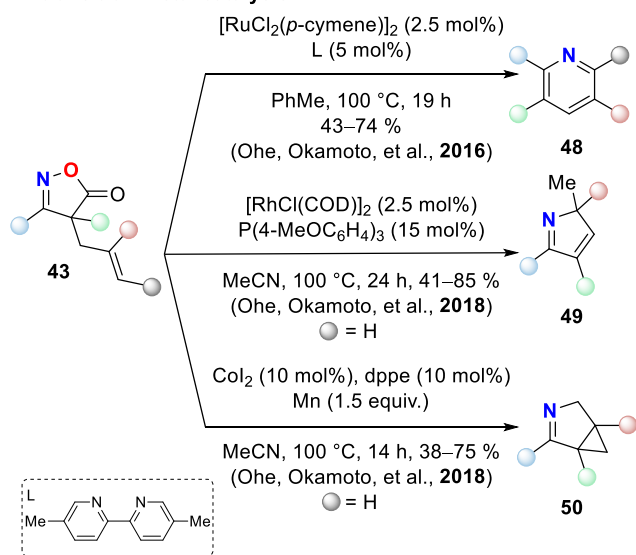
Scheme 11. a) Decarboxylative aziridination of *4H*-isoxazol-5-ones; b) Mechanistic proposal based on DFT calculations (only the main intermediates are drawn).

Careful choice of the metal/ligand system coupled with different substituents on the substrate can vastly influence the outcome of such transformations. In a follow-up study, Ohe et al. were able to streamline this idea further and use the same class of substrates to access highly substituted pyridines **48**.<sup>[55]</sup> The authors suggested that a Ru-ketimido complex was a possible intermediate species, as in the case of oxime esters (Scheme 3e).<sup>[13]</sup> Interestingly, in the presence of Rh- or Co-catalysts, the same starting materials gave *2H*-pyrroles **49** and azabicyclic cyclopropanes **50**, respectively (Scheme 12a).<sup>[56]</sup> Li et al. conducted an in-depth DFT analysis of the Rh- and Co-catalytic

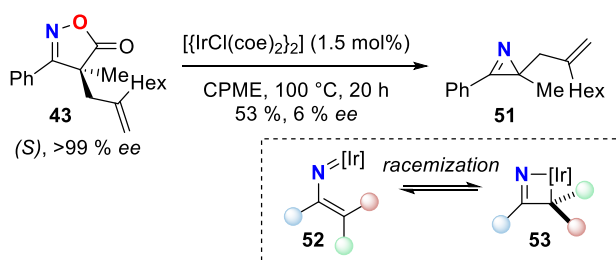
systems. They found that the selectivity is mainly influenced by the respectively different geometries of Rh(I) and Co(II) key catalytic species, which is in line with the usually favored geometries of the respective systems. According to the computational results, the insertion of the olefin precedes decarboxylation, as opposed to what was initially expected by the authors.<sup>[57]</sup> These findings could also explain why no intermolecular version of these reactions is reported up-to-date.

Under decarboxylative reaction conditions with the aid of an Ir(I) catalyst, it is also possible to synthesize the ring-contraction products, *2H*-azirines **51**. Here, the chiral information is not transferred to the product. This observation is highly suggestive of a metallanitrene intermediate, as the equilibrium between the vinyl nitrene **52** and iridacycle **53** can account for the racemization of the substrate (Scheme 12b).<sup>[58]</sup>

**a) Divergent transformations of 4*H*-isoxazole-5-ones under transition-metal catalysis**



**b) Synthesis of 2*H*-azirines and loss of chiral information**  
(Ohe, Okamoto, et al, 2016)

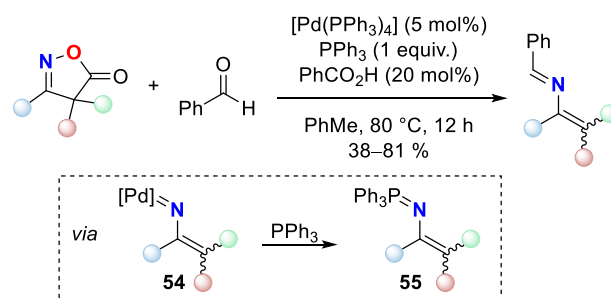


Scheme 12. Divergent reactivity of 4*H*-isoxazol-5-ones under various catalysis: a) Synthesis of highly substituted pyridines under Ru(II)-catalysis, 2*H*-pyrroles formation under Rh(I)-catalysis, and Co(II)-catalyzed formation of azabicyclic cyclopropanes; b) 2*H*-Aziridines obtained under Ir(I)-catalysis and explanation of the racemization process. COD = 1,5-cyclooctadiene; dppe = 1,2-bis(diphenylphosphino)ethane; coe = cyclooctene; CPME = cyclopentyl methyl ether.

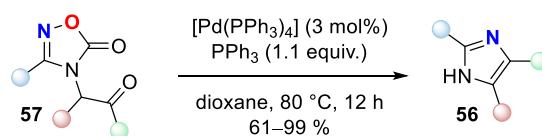
Putative Pd(II)-nitrene intermediates can also engage in aza-Wittig-type reactions that lead to iminophosphoranes. Here, the generated nitrenoid **54** is supposed to transfer nitrene to the phosphine. This method has the benefit that no explosive azides are used, in contrast to the traditional generation of iminophosphoranes in the Staudinger reaction. To activate the aldehyde, catalytic amounts of benzoic acid were required. The need for a stoichiometric amount of triphenylphosphine suggests

that the transformation proceeds via an iminophosphorane of type **55**. One equivalent of triphenylphosphine is necessary, as an oxidation event consumes it during the aza-Wittig reaction (Scheme 13a).<sup>[59]</sup> This transformation is not limited to the aldehyde, as well as to the heterocyclic partner. Ohe, Okamoto et al. have also reported the synthesis of imidazoles **56** in an equivalent manner by using diazoles **57** (Scheme 13b).<sup>[60]</sup> This method of generating metallanitrenes has the potential to be further developed and extended to different classes of iminophosphoranes.

**a) Aza-Wittig reaction** (Ohe, Okamoto, et al., 2014)



**b) Synthesis of imidazoles** (Ohe, Okamoto, et al., 2014)

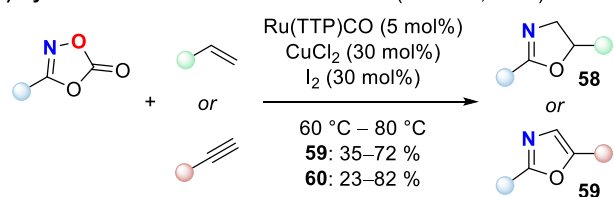


Scheme 13. Synthetic methodologies going through an iminophosphorane intermediate under Pd-catalysis: a) Aza-Wittig type reaction starting from 4*H*-isoxazol-5-ones; b) Synthesis of imidazoles from oxadiazolones.

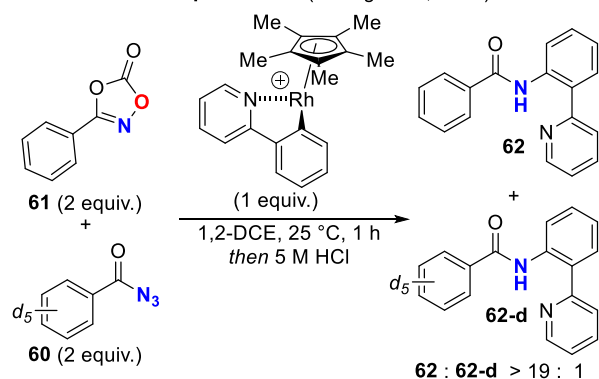
Along with isoxazolones, dioxazolones easily obtained from the corresponding carboxylic acids have been known since the 60s as readily accessible nitrene precursors.<sup>[46]</sup> However, their use as metallanitrene precursors dates back to the beginning of the 2010s when He et al. demonstrated that both oxazolines **58** and oxazoles **59** could be readily synthesized in the presence of a Ru-based catalyst from dioxazolones and alkynes or alkenes, respectively (Scheme 14a).<sup>[61]</sup> Even if the involvement of a metallanitrene intermediate was highly probable, no experimental proof was given in this seminal study.

Chang, Kim et al. later provided such proof, revealing that dioxazole derivatives lead more easily to nitrenes than the traditionally-used azides. The difference in reactivity between dioxazoles and azides was demonstrated by subjecting a mixture of these two classes of compounds to a stoichiometric amount of a cationic Rh(III)-complex to perform a C–H amidation. In a competition reaction, when only the phenyl moiety of the azide partner **60** was labeled with deuterium, contrary to the substituted 1,4,2-dioxazole-5-one **61**, it was noted that the non-labeled product **62** forms in a significant excess (**62**: **62-d**>19:1, Scheme 14b). To explain this reactivity, the authors performed DFT calculations, showing that the formation of the metallanitrene intermediate was more favorable in the case of the carbon dioxide expulsion, i.e., in the case of dioxazole derivatives **61** – as compared to the azides **60** ( $\Delta\Delta G^\ddagger=12.7 \text{ kcal}\cdot\text{mol}^{-1}$ ). The authors also demonstrated that dioxazoles **63** and arenes **64** could be successfully reacted to achieve the Rh-catalyzed C–H amidation. An important example from this publication is a gram-scale amidation of arene **65**, where a pyridyl directing group allows for a selective C–H amidation in the *ortho* position (Scheme 14c).<sup>[62]</sup>

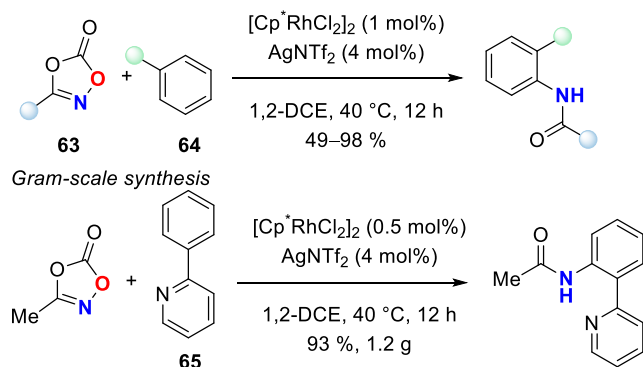
**a) Synthesis of oxazolines and oxazoles** (He et al., 2012)



**b) Competitive reactivity between dioxazolones and azides as metallanitrene precursors** (Chang et al., 2015)



**c) Rh-catalyzed C–H amidations** (Chang et al., 2015)

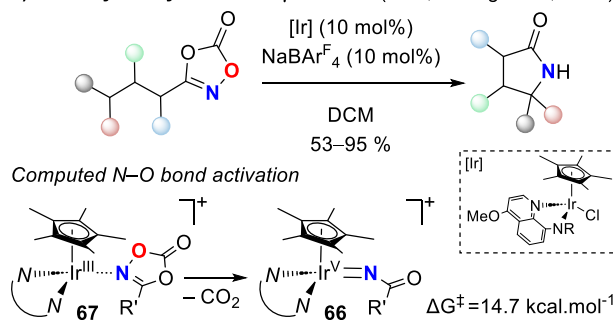


Scheme 14. Dioxazolones as metallanitrene precursors: a) Ru-catalyzed synthesis of oxazolines and oxazoles from dioxazolones via amino-oxygenation of alkenes and alkynes, respectively; b) Competition reaction between azides and dioxazolones under Rh-catalysis; c) Rh-catalyzed C–H amidation reactions with dioxazolones as metallanitrene precursors. TPP = 5,10,15,20-tetraphenyl-21*H*,23*H*-porphine; 1,2-DCE = 1,2-dichloroethane.

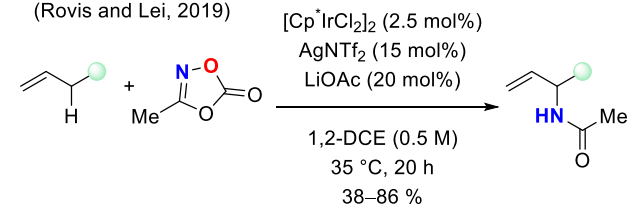
Baik, Chang et al. used the same mechanistic rationale to develop an Ir-catalyzed intramolecular C–H amidation toward synthesizing  $\gamma$ -lactams. Although no experimental proof was given, the reaction's outcome was consistent with the involvement of an Ir-nitrene intermediate. DFT calculations confirmed that Ir(V)-nitrene intermediate **66** was indeed energetically accessible under the reaction conditions ( $\Delta G^\ddagger=14.7$  kcal.mol<sup>-1</sup> from the Ir(III)-dioxazolone complex **67**, Scheme 15a).<sup>[49c]</sup>

During the last several decades, dioxazolones have proven their versatility as a novel class of C–H amidating reagents through a metallanitrene intermediate. Directing groups are required most of the time, and a large variety has been utilized in this transformation, such as thioamides,<sup>[63]</sup> fused azoles,<sup>[64]</sup> oxazolynyl- moiety,<sup>[65]</sup> and anilides.<sup>[66]</sup> Rovis and Lei developed the branch-selective allylic C–H amidation, which proceeds via Ir(III) catalysis without a directing group. Here an allyl-Ir(III) intermediate further participates in the oxidative amidation to give an amide at the branched position of a terminal alkene (Scheme 15b).<sup>[67]</sup>

**a) Ir-catalyzed synthesis of  $\gamma$ -lactams** (Baik, Chang et al., 2018)



**b) Ir-catalyzed C–H amidation with different branched alkenes** (Rovis and Lei, 2019)

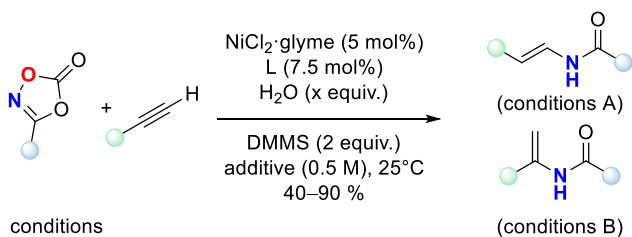


Scheme 15. Ir-catalyzed reaction with dioxazolones as metallanitrene precursors: a) Synthesis of  $\gamma$ -lactams and computed N–O bond activation by Ir(III)-intermediate **67**; b) C–H amidation with branched alkenes. 1,2-DCE = 1,2-dichloroethane.

Bolm and Hermann showed that it is possible to perform a ball-milling Rh(III)-catalyzed amidation of arenes under solvent-free conditions.<sup>[68]</sup> Bolm et al. also reported the amidation of sulfides using [Ru(TPP)CO] (TPP = 5,10,15,20-tetraphenyl-21*H*,23*H*-porphine) as the catalyst under irradiation with a high-pressure Hg-lamp.<sup>[69]</sup>

The metallanitrenes generated from dioxazolones can even be engaged in cascade reactions, e.g., for the hydroamidation of alkynes in the presence of a Ni-catalyst, as described by Seo, Chang et al. The fine-tuning of the reaction conditions allows the regioselectivity to be controlled toward either the anti-Markovnikov or the Markovnikov product. Seo, Chang et al. provided evidence for a Ni(III)-nitrene intermediate by demonstrating its capture with PPh<sub>3</sub> as an imidophosphorane. They also performed DFT computations, which confirmed that Ni(III)-intermediate **68** was energetically accessible ( $\Delta G^\ddagger=10.8$  kcal.mol<sup>-1</sup> from the Ni(I)-complex **69**, Scheme 16a).<sup>[70]</sup> Rovis and Lee also developed a three-component Rh(III)-catalyzed *syn*-carboamination of alkenes by employing dioxazolones and aryl boronic acids (Scheme 16b).<sup>[71]</sup>

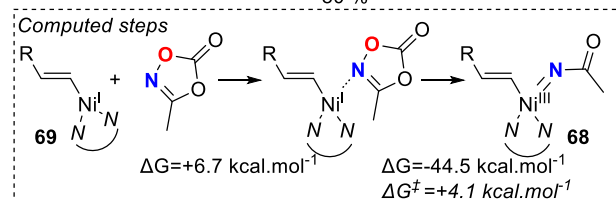
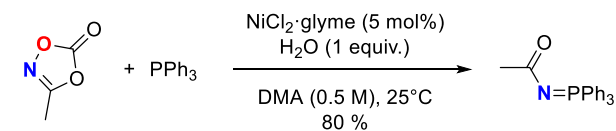
### a) Hydroamidation of alkynes (Seo, Chang et al., 2021)



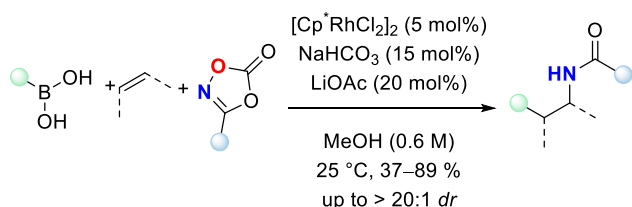
conditions

A: additive = DMA; L = 2,2'-bipyridine; x = 0.6

B: additive = DMPU; L = 6,6'-di-*sec*-butyl-2,2'-bipyridine; x = 1.0



### b) Three-component *syn* carboamination (Rovis and Lee, 2021)



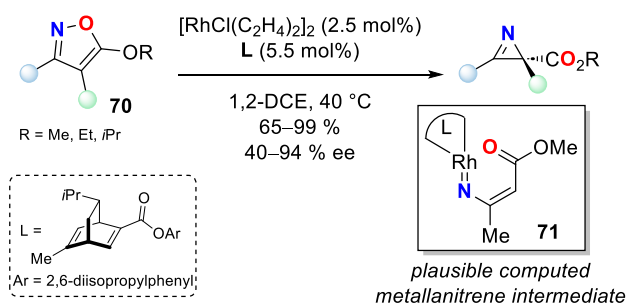
Scheme 16. Selected examples of the reactivity of dioxazolone-derived nitrene species engaged in cascade reactions: a) Hydroamidation of alkynes under Ni-catalysis and computed N–O bond activation; b) Three-component carboamination of olefins under Rh-catalysis. DMMS = dimethoxymethylsilane; DMA = *N,N*-dimethylacetamide; DMPU = *N,N'*-dimethylpropyleneurea.

The variety of described conditions further solidifies the potential of isoxazoles and dioxazolones as metallanitrene precursors: by controlling the reactivity, one can effectively construct a C–N bond selectively.

### 3.2. Non-decarboxylative transformation leading to nitrene intermediates

Other compounds containing an N–O bond can be downstreamed into synthetically highly appealing products via metallanitrene intermediates.

Inspired by their studies on dioxazolones (*vide supra*), Okamoto, Ohe et al. have designed an asymmetric synthesis of 2*H*-azirines from isoxazoles **70**. According to preliminary mechanistic studies, a rhodium-imido intermediate **71**, resulting from the N–O bond cleavage, would explain the observed reactivity (Scheme 17).<sup>[72]</sup>

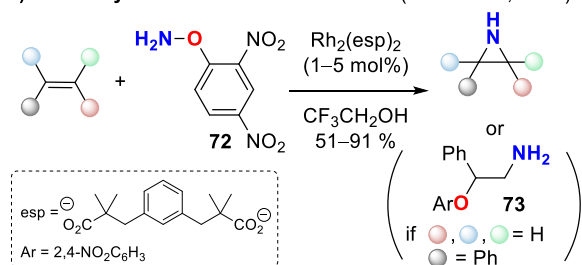


Scheme 17. Asymmetric synthesis of 2*H*-azirines by Ohe, Okamoto, et al. from isoxazoles and computed rhodium-imido intermediate.

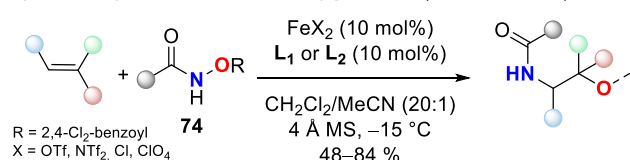
Simple hydroxylamines can also lead to metallanitrene intermediates. Falck et al. first reported a rhodium-catalyzed synthesis of aziridines from alkyl-substituted alkenes starting with *O*-(2,4-dinitrophenyl)hydroxylamine (**72**) as the aminating reagent. The involvement of a metallanitrene intermediate was suggested by DFT computations. In the case of styrenyl derivatives, even the oxygen-containing part of the hydroxylamine was incorporated into the molecule, leading to the 1,2-amino-alcohol product **73**, presumably resulting from the ring opening of an aziridine intermediate (Scheme 18a).<sup>[73]</sup>

Olefin difunctionalization is a synthetically economic process. Traditionally, enantioselective olefin amino-oxygenations are performed via Sharpless epoxidation. This reaction implies using non-precious metals with a strong oxidant – typically peroxides such as *t*BuOOH. Xu et al. reported an intramolecular Fe(II)-catalyzed amino-oxygenation of olefins with *N*-protected hydroxylamines **74**. Interestingly, the hydroxylamine derivative acts as an internal oxidant and a source of amine and alcohol. A tridentate ligand (**L**<sub>1</sub> or **L**<sub>2</sub>) is crucial for a successful transformation. The method even proved effective in the diastereoselective synthesis of an amino sugar from a protected glycal (Scheme 18b). The exact mechanism of this transformation remains unknown. However, radical clock experiments showed a positive result. Moreover, the rearrangements observed in the reaction starting with 2,3-dimethylbut-1-ene hinted at a carbocation intermediate. The authors thus suggested a stepwise transformation that goes through a radical amination step, followed by the formation of a carbocation intermediate (Scheme 18c).<sup>[74]</sup> The radical pathway proposed here is consistent with the expected behavior of the iron-stabilized nitrene.<sup>[51a,75]</sup>

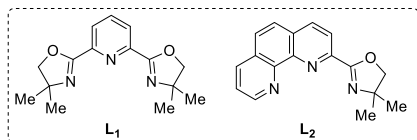
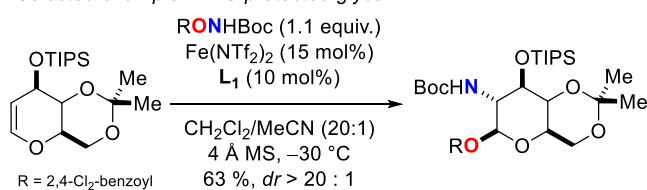
**a) Rh-catalyzed aziridination of alkenes** (Falck et al., 2014)



**b) Fe-catalyzed olefin amino-oxygenation** (Xu et al., 2014)

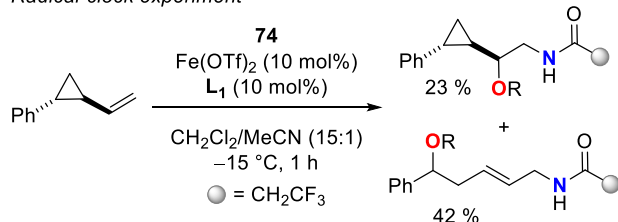


Selected example: TIPS-protected glycol

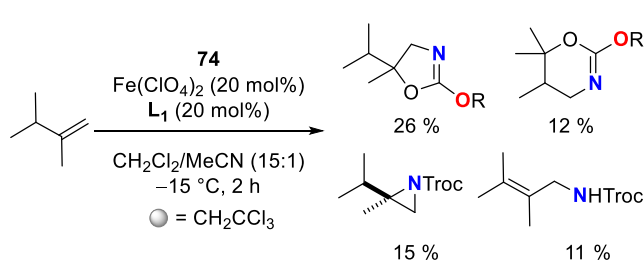


**b) Experimental proofs for a Fe-nitrene pathway** (Xu et al., 2014)

Radical-clock experiment



Hint for a carbocation intermediate



Scheme 18. Reaction involving a putative nitrenoid intermediate generated from hydroxylamine derivatives: a) Rh-catalyzed aziridination of alkenes; b) Fe-catalyzed olefin amino-oxygenation and application to a TIPS-protected glycol; c) Mechanistic experiments hinting at an iron-nitrene pathway. Troc = 2,2,2-Trichloroethoxycarbonyl.

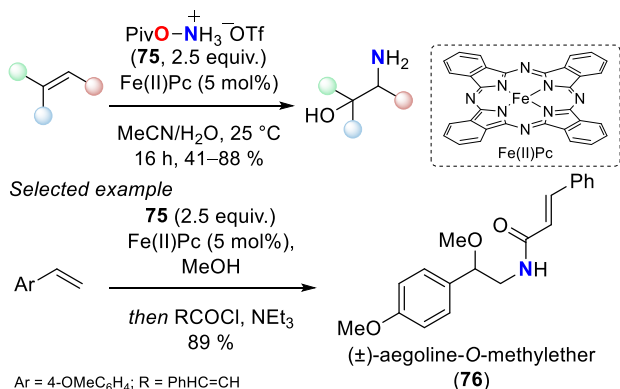
Morandi and Legnani have reported using the bench-stable nitrogen source PivONH<sub>3</sub>OTf (**75**) to access unprotected primary amines directly. In the presence of O-nucleophiles (MeOH, higher order alcohols, or water) and a Fe(II)-phthalocyanine (Pc) catalyst, olefins underwent amino-oxygenation. This approach provides novel access to multiple active molecules, for example, the natural antibacterial product **76** obtained as a racemic mixture (Scheme 19a).<sup>[76]</sup> This concept was further applied to amino-

chlorination,<sup>[77]</sup> amino-azidation,<sup>[78]</sup> and the synthesis of sulfur-containing compounds.<sup>[79]</sup>

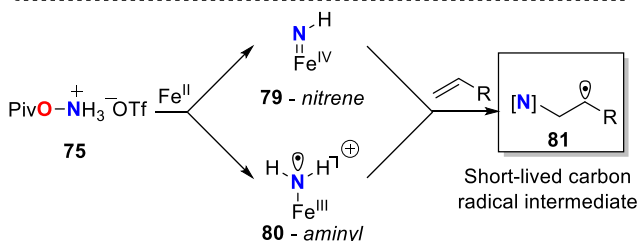
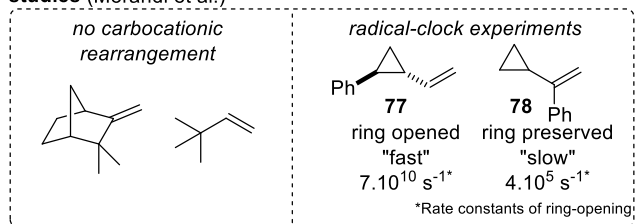
From a mechanistic point of view, the involvement of a carbon-centered radical intermediate in these reactions is suggested by the absence of an alkyl shift in the reaction with camphene<sup>[77a]</sup> or 3,3-dimethyl-1-butene.<sup>[78]</sup> Different radical clock experiments have further proven that this carbon-centered radical must be short-living. Indeed, the fast radical clock **77** ( $k = 7.10^{10} \text{ s}^{-1}$ ) underwent ring-opening, whereas the slower **78** ( $k = 4.10^5 \text{ s}^{-1}$ ) did not.<sup>[76-78]</sup> Although the yields dropped in the presence of radical scavengers (TEMPO, BHT), no adduct was obtained.<sup>[77a,78]</sup> These experiments highlight the significant influence of kinetics in trapping radical intermediates, particularly when they are short-living. The absence of a ring-opened product does not always mean that no radical intermediates are involved. Based on the above experiments, Morandi et al. proposed two mechanistic pathways involving either a Fe(IV)-nitrene complex **79** or a Fe(III)-aminyl complex **80** as an intermediate. In both cases, their addition to the olefin should lead to a carbon-centered radical intermediate **81** (Scheme 19b).

Although the exact mechanism of the amino-functionalization with PivONH<sub>3</sub>OTf (**75**) is still controversial, recent advanced spectroscopic and computational mechanistic studies show a dramatic effect of the ligand on the reaction pathway. Both N–O bond homolysis and heterolysis have been proposed with [Fe(acac)<sub>2</sub>(H<sub>2</sub>O)<sub>2</sub>] (acac=acetylacetonate)<sup>[80]</sup> and [Fe(II)Pc]<sup>[81]</sup> as catalysts, respectively. In the first case, a high-spin iminyl radical species Fe(III)–NH• **82** is assumed to be directly formed from **75**.<sup>[80]</sup> In contrast, a cationic iron-amido complex Fe(III)–NH<sub>2</sub><sup>+</sup> **83** is presumed to be the catalytic intermediate in the latter, allowing the use of the O-acetate hydroxylamine salt **84** (Scheme 19c).<sup>[81]</sup> Both studies, however, ruled out the involvement of a true nitrene intermediate of type **79** and confirmed the participation of a carbon-radical intermediate **81**.

**a) Fe(II)-phthalocyanine catalyzed synthesis of amino alcohols**  
(Morandi and Legnani, 2016)



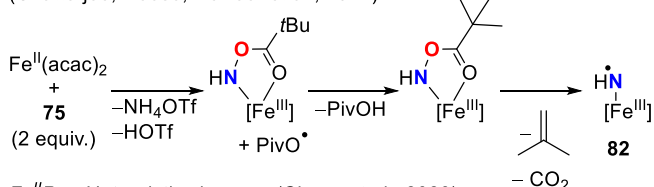
**b) Proposed mechanism based on preliminary mechanistic studies** (Morandi et al.)



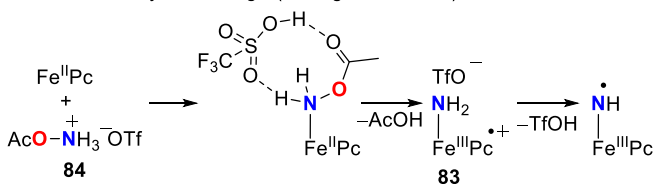
**c) Proposed mechanisms for the N–O bond cleavage based on advanced mechanistic studies (spectroscopic & computational)**

*Fe<sup>II</sup>(acac)<sub>2</sub> - Homolytic cleavage*

(Chatterjee, Neese, DeBeer et al., 2022)



*Fe<sup>II</sup>Pc - Heterolytic cleavage* (Cheng et al., 2023)



Scheme 19. a) Iron(II)-catalyzed synthesis of amino alcohols and application to the synthesis of a natural antibacterial natural product; b) Preliminary mechanistic studies and initial mechanism proposed; [76-78] c) Mechanisms proposals based on advanced mechanistic studies. acac = acetylacetonate.

Under certain conditions, N–O bond activation with different transition metals can thus lead to highly reactive metallanitrene intermediates, as demonstrated in this Section. Various reactivities can therefore be accessed by carefully choosing the reaction parameters, i.e., C–H amidation, alkene (di)functionalization, and ring contraction.

## 4. Nitrogen-centered radicals generation from N-oxides

Inspired by Barton and Tsuchiya's reactions, many studies have recently been published that use the low BDE of the N–O bond (Scheme 1).<sup>[6-7]</sup> Most of these reactions rely on the use of specific nitrogen substituents acting as electrophores, especially oxime esters<sup>[82]</sup> and the so-called "redox active esters"<sup>[83]</sup> inspired by the works of Barton (thiohydroxamate esters)<sup>[6]</sup> and Okada (*N*-hydroxyphthalimides derivatives).<sup>[84]</sup> Thermal,<sup>[85]</sup> photochemical,<sup>[86]</sup> and electrochemical activations<sup>[87]</sup> have been employed to break the N–O bond, either homolytically or via single electron transfer (generating either nitrogen or oxygen radicals). Recently, the groups of Cho and Glorius independently showed that oxime esters could also undergo energy transfer from a photoexcited catalyst and generate both nitrogen- and oxygen-centered radicals.<sup>[88]</sup>

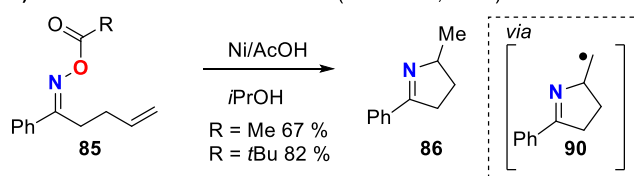
Among the reported methodologies, the use of single electron transfer (SET) from an (organo)metallic compound has been developing quickly. This third part will focus on the generation and use of nitrogen radicals<sup>[89]</sup> generated through single electron transfer from a metallic species, and we will highlight the experimental proofs for a radical mechanism.

### 4.1 Stoichiometric reactivity

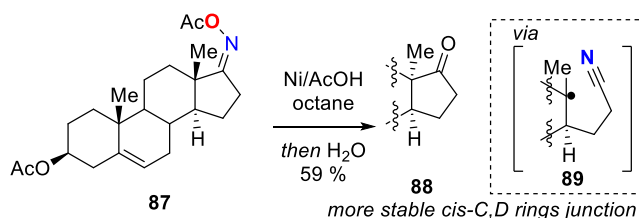
Zard et al. reported the seminal examples of SET to an N–O bond from a metallic species. They showed that oxime esters **85** could be singly reduced with a stoichiometric amount of Ni powder in the presence of acetic acid using isopropanol as a solvent. Other plain metals proved less efficient, as the second reduction to the imine anion is much faster. With Ni(0) the resulting nitrogen radical was sufficiently long-lived to undergo intramolecular 5-exo cyclization with a pendant alkene. Under these conditions, dihydropyrroles such as compound **86** formed. Acetate and pivalate derivatives **85** were tested, with the latter determined as more robust toward premature hydrolysis of the oxime ester (82 % yield vs. 67 % with acetate) (Scheme 20a).<sup>[90]</sup>

From a mechanistic point of view, the reduction could have also led to a carboxylic radical RCOO•, which would then undergo a fast decarboxylation. However, no side-products could be detected. The epimerization of 17-ketosteroid oxime derivative **87** via D-ring opening/closing represents a mechanistic proof for an iminyl radical intermediate. Indeed, the more stable 13-epi-17-ketosteroid **88**, where the C–D ring junction is *cis*, was the major product of the reaction after hydrolysis. The stereochemistry inversion resulted from a ring opening of the 17-iminyl radical intermediate that formed the tertiary radical **89**. Radical **89** cyclized to give the more stable *cis*-junction, which explains why ketosteroid **88** was obtained after hydrolysis (Scheme 20b). The authors explained that the solvent (isopropanol) was thus a hydrogen donor in the reaction.<sup>[90a]</sup> The resulting carbon-centered radical **90** reacted with other radical traps, such as diphenyl diselenide or allyl tolyl sulfones, leading to the amino-selenation or amino-vinylation reactions, respectively.<sup>[90b]</sup>

a) Ni as stoichiometric reductant (Zard et al., 1992)



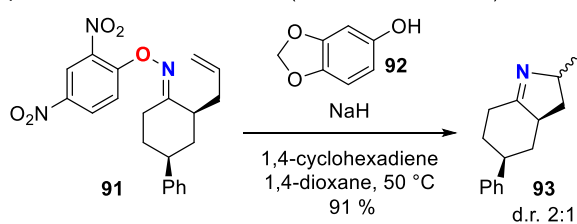
b) Estrone epimerization – hint for a radical mechanism



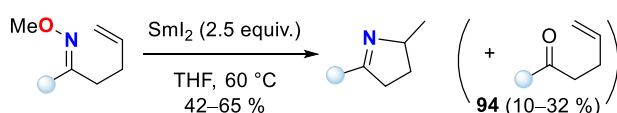
Scheme 20. a) Reduction of oxime esters with stoichiometric Ni(0) toward synthesizing dihydropyrroles; b) Epimerization of a ketosteroid derivative as radical mechanistic proof.

In the meantime, Narasaka et al. disclosed the synthesis of dihydropyrroles from *O*-2,4-dinitrophenyl oximes **91** in the presence of phenol **92** and NaH. The reaction was believed to start with a single electron transfer from the phenolate to the dinitrophenyl substituent, playing the role of an electrophore. The subsequent formation of an iminyl radical intermediate via homolytic scission of the N–O bond was suggested. According to the authors, the favored 5-exo over the 6-endo cyclization, leading to dihydropyrrole **93** with a 2:1 diastereomer ratio, confirmed a radical pathway (Scheme 21a).<sup>[95b]</sup> More recently, Zhang et al. showed that 2.5 equivalents of Sml<sub>2</sub> could also trigger the formation of an iminyl radical from methoxy oxime ethers. However, the formation of the imine anion resulting from a second reduction with Sml<sub>2</sub> could not be wholly suppressed, leading to the formation of ketone **94** in significant amounts (Scheme 21b).<sup>[91]</sup>

a) NaH/*m*-cresol as reductant (Narasaka et al., 1998)



b) Sml<sub>2</sub> as reductant (Zhang et al., 2019)

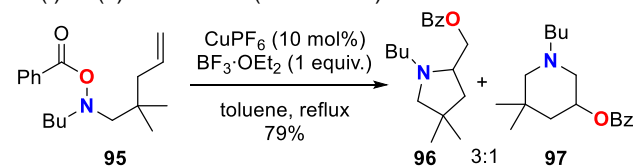


Scheme 21. Synthesis of dihydropyrroles from oximes via a supposed radical mechanism: a) from *O*-2,4-dinitrophenyl oximes through reduction with phenol **92** and NaH; b) from methoxy oxime ethers in the presence of stoichiometric Sml<sub>2</sub>.

## 4.2. Cu-catalyzed reactions

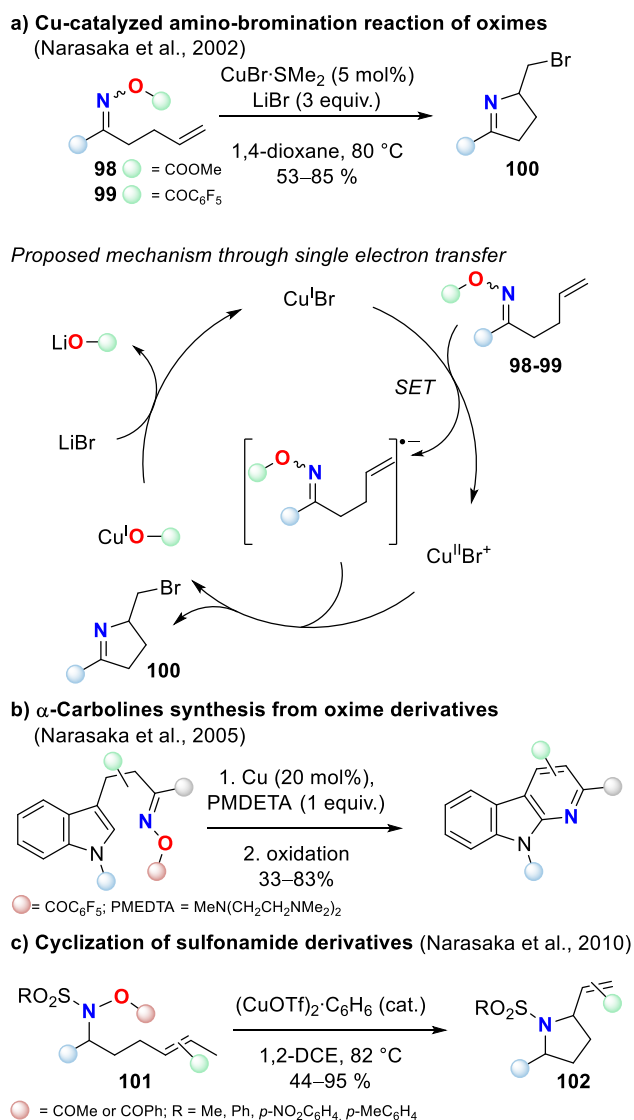
In 2002, Göttlich et al. disclosed a Cu-catalyzed pyrrolidine synthesis from *O*-benzylated hydroxylamines **95**. A stoichiometric amount of BF<sub>3</sub>·OEt<sub>2</sub> drastically improved the yield of the reaction, certainly by coordinating the benzoyl group and thus destabilizing the N–O bond. The amino and the benzoyl parts were transferred

in the final molecule, leading to an amino-oxygenation of the alkene. According to the authors, the major formation of the 5-membered ring **96** over the 6-membered **97** supported the hypothesis of an aminyl radical intermediate, therefore of a Cu(I)/Cu(II) mechanism (Scheme 22).<sup>[92]</sup>



Scheme 22. Pyrrolidine synthesis via intramolecular aminohydroxylation reactions under Cu(I)-catalyzed conditions described by Göttlich et al.

The same year, Narasaka et al. reported that CuBr·SMe<sub>2</sub> could catalyze the cyclization reaction of oxime esters. *O*-methoxycarbonyl- **98** and *O*-pentafluorobenzoyl oximes **99** both underwent efficient cyclization. Adding LiBr improved the cyclization efficiency and led to brominated dihydropyrroles **100**. Although a radical pathway was proposed, no direct proof was given (Scheme 23a).<sup>[93]</sup> The strategy was applied to the synthesis of cyclic imines and  $\alpha$ -carboline derivatives (Scheme 23b).<sup>[94]</sup> Additionally, the group extended the reaction to *N*-alkenyl *N*-benzoyl sulfonamides **101** toward synthesizing pyrrolidines **102** (Scheme 23c). Again, a radical mechanism was proposed since the 5-membered ring was obtained as the major product, if not the only one.<sup>[95]</sup>



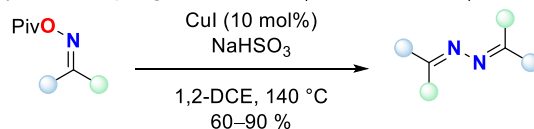
Scheme 23. a) Cu-catalyzed amino-bromination reaction of oxime derivatives and proposed mechanism via a single electron transfer step explaining the observed reactivity; b) Example of Cu-catalyzed synthesis of  $\alpha$ -carbolines from oximes; c) Extension of the reaction to sulfonamide derivatives.

Experimental proofs for a radical pathway in the reaction of copper(I) salts and oxime esters have only been disclosed recently. Ten years after the seminal communications, the reported homocoupling of oxime esters under Cu(I)-catalysis brought another argument for the involvement of radical events (Scheme 24a).<sup>[96]</sup> In 2014, Bower et al. reported a Cu-catalyzed intramolecular Heck-like reaction starting from *O*-pivaloyl and *O*-acetyl oxime esters **103**. Mechanistic investigations revealed that the alkene did not react via migratory insertion in the Cu–N bond but most likely via adding the iminyl radical intermediate **104**. The latter was formed either by SET from Cu(I) to the oxime ester or through the homolytic scission of a Cu(III)–N bond. Evidence of a copper(I) species was given by the formation of a characteristic deep-purple Cu(I)-cuproin complex when cuproin was added under the reaction conditions. The estrone epimerization and radical clock experiments confirmed the involvement of iminyl and alkyl radical intermediates **104** and **105**, respectively (Scheme 24b).<sup>[97]</sup>

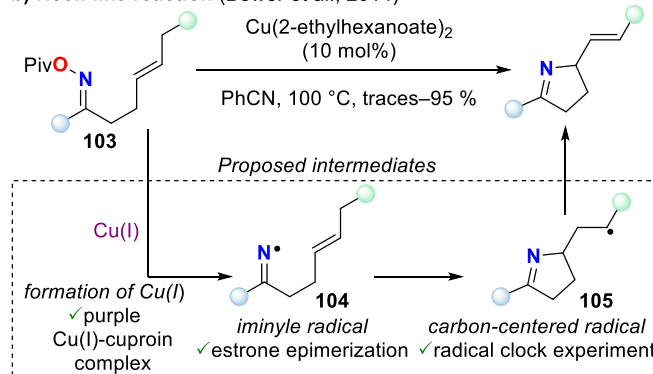
One year later, Lei et al. demonstrated by EPR spectroscopy the presence of copper(II) salts when *O*-acetyl oxime **106** reacted with CuCl. In the presence of 5,5-dimethyl-1-pyrroline *N*-oxide

(**107**, DMPO) as a radical trap, adduct **108** was detected, suggesting that an iminyl radical was formed in the process (Scheme 24c).<sup>[98]</sup> Wang et al. reported a Cu-catalyzed imino-amination reaction, which corresponded to the difunctionalization of an alkene with a pendant oxime ester and an external amine. The authors also proposed that the transformation was following a radical pathway. Their hypothesis was based on the in-situ trapping reaction with (2,2,6,6-tetramethylpiperidin-1-yl)oxyl (TEMPO), which led to the adduct **109**. The reaction with substrate **110** confirmed the hypothesis since only ring-opened products **111** and **112** were observed (Scheme 24d).<sup>[99]</sup>

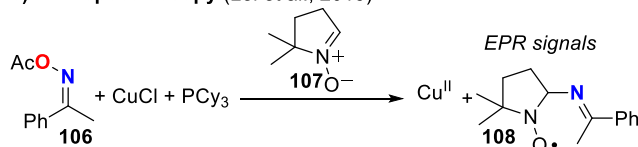
**a) Homocoupling of ketoximes** (Guan et al., 2012)



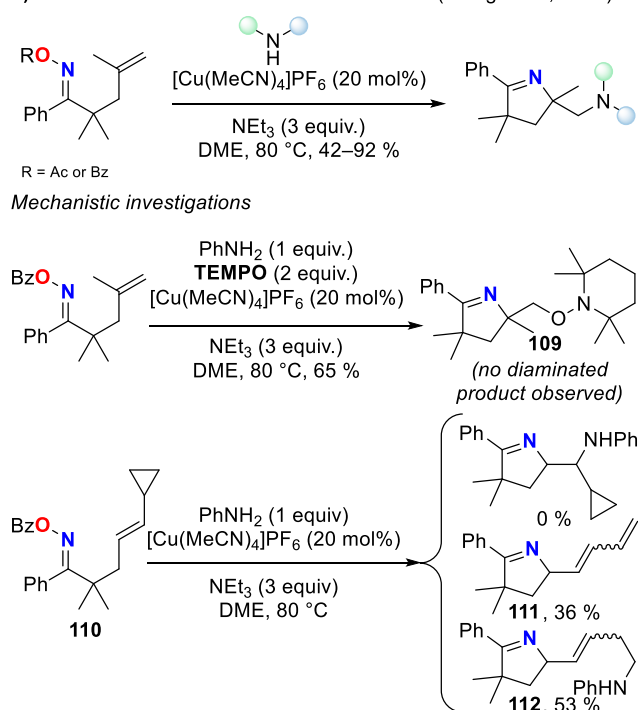
**b) Heck-like reaction** (Bower et al., 2014)



**c) EPR spectroscopy** (Lei et al., 2015)



**d) Imino-amination of alkenes from oximes** (Wang et al., 2019)

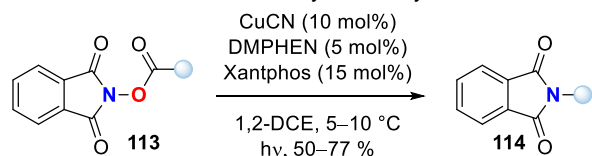


Scheme 24. Experimental proofs for iminyl and carbon-centered radicals intermediates in the presence of Cu-catalysts: a) Homocoupling of ketoximes;

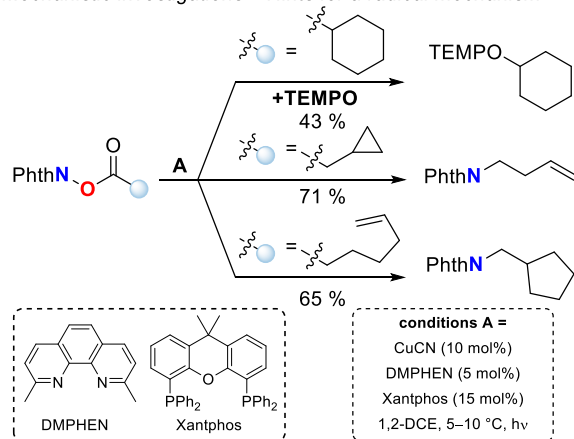


b) Proposed radical intermediates in the Heck-like reaction with the corresponding experimental proofs (Cu(I)-cuproin complex, estrone epimerization, and radical clock experiment); c) Trapping with DMPO of the iminyl radical observed by EPR spectroscopy; d) Imino-amination reaction and corresponding mechanistic investigations. DMPO = 5,5-dimethyl-1-pyrroline *N*-oxide; TEMPO = (2,2,6,6-tetramethylpiperidin-1-yl)oxyl; DME = dimethylether.

Fu, Peters et al. disclosed an interesting example in 2017. Under light irradiation and in the presence of CuCN, neocuproine (DMPHEN), and Xantphos, *N*-hydroxy phthalimide (NHP) esters **113** led to protected amines **114**. Upon excitation of a copper(I) species, this contraction reaction is believed to result from a single electron transfer to the NHP ester, forming a phthalimidate ligand and a carboxyl radical, which undergoes fast decarboxylation. Trapping experiment with TEMPO and radical clock hinted at a radical mechanism (Scheme 25). The authors showed that the reaction worked more efficiently with primary carboxylic acid derivatives than with secondary or tertiary ones.<sup>[100]</sup>



Mechanistic investigations – Hints for a radical mechanism



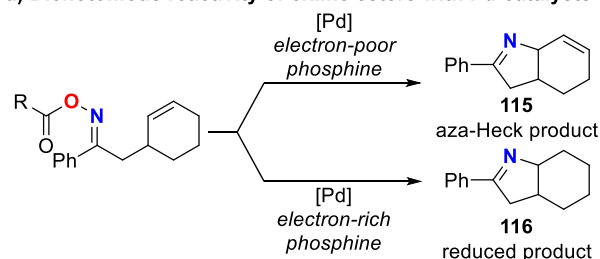
Scheme 25. Contraction reaction as described by Fu, Peters, et al. with experimental proofs for a radical mechanism. 1,2-DCE = 1,2-dichloroethane; TEMPO = (2,2,6,6-tetramethylpiperidin-1-yl)oxyl.

### 4.3. Pd dichotomous reactivity

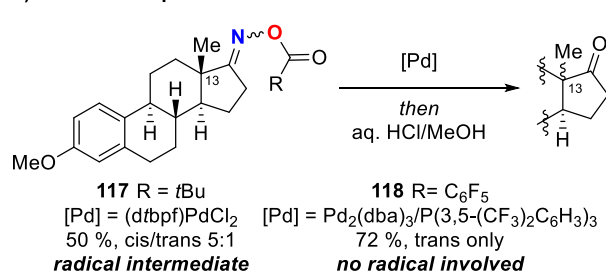
During their study on Pd-catalyzed Narasaka-Heck cyclization, Bower et al. serendipitously found a dichotomous reactivity of [Pd] catalysts, depending on the nature of the phosphine ligands. Whereas electron-poor phosphines favored the typical oxidative addition and the aza-Heck product **115** (see before), electron-rich phosphines (typically SPhos, P(*t*Bu)<sub>3</sub>, P(Cy)<sub>3</sub> and PEPPSI-IPR as ligands led to the reduced product **116** (Scheme 26a).<sup>[29]</sup> The authors then hypothesized that a radical pathway was involved. Introducing sacrificial hydrogen donors such as 1,4-cyclohexadiene and  $\delta$ -terpinene improved the reaction efficiency, whereas proton donors such as formic acid did not change the reaction outcome, suggesting a radical intermediate. The radical clock opening and a trapping reaction with TEMPO further hinted at the radical pathway. Inspired by the work of Zard (Scheme 20),<sup>[90]</sup> a final experiment using oxime estrones **117** and **118** was performed. When the electron-rich phosphine ligand 1,10-bis(di-*tert*-butylphosphino)ferrocene (dtbpf) was used,

epimerization of carbon 13 was observed, demonstrating a radical pathway. In contrast with the electron-poor phosphine ligand P(3,5-(CF<sub>3</sub>)<sub>2</sub>C<sub>6</sub>H<sub>3</sub>)<sub>3</sub>, no epimerization could be detected (Scheme 26b).<sup>[29]</sup> This result shed light on the mechanistic pathway of the oxidative addition toward synthesizing Hartwig's and Stahl's complexes **23** and **26** bearing electron-rich phosphine ligands (PCy<sub>3</sub>, Scheme 5).<sup>[27–28]</sup> According to Bower's findings, their formations indeed went via a single electron transfer from Pd(0) to the oxime ester, followed by recombination of the iminyl radical and the Pd(I) instead of the classical 3-centered oxidative addition.

#### a) Dichotomous reactivity of oxime esters with Pd-catalysts



#### b) Mechanistic proof for two different mechanisms

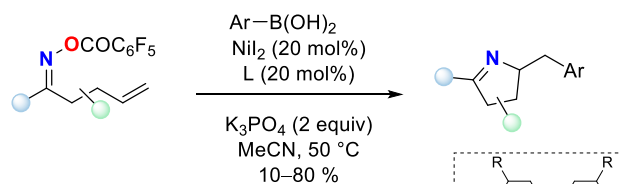


Scheme 26. Pd-catalyzed reactions of oxime esters reported by Bower et al.: a) Dichotomous reactivity of oxime esters in the presence of Pd-catalyst depending on the electronic of the phosphine ligand; b) Estrone mechanistic proof for two different mechanisms involving either a radical or a polar mechanism.

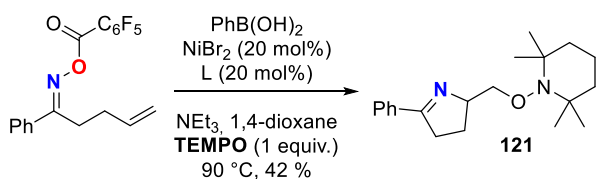
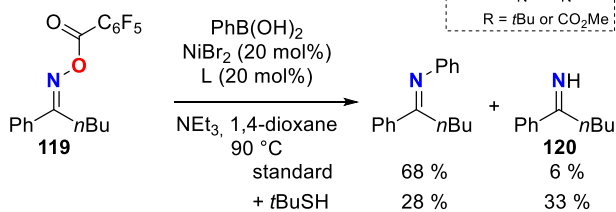
### 4.4. Ni and Fe catalyzed reactions: amino-arylation and -alkynylation

Inspired by the work of Bower on palladium catalysis, Selander et al. disclosed a Ni-catalyzed 1,2-aminoarylation. Here, the cyclization of the oxime ester is followed by a direct cross-coupling with an aryl boronic acid (Scheme 27a). The motivation for using a Ni(II) salt was to avoid the  $\beta$ -hydride elimination regularly encountered with Pd-catalysis and facilitate the cascade post-functionalization. Reacting saturated oxime ester **119** with phenyl boronic acid under the standard conditions in the presence of *tert*-butylthiol as a hydrogen donor resulted in an increased yield of the NH-imine **120**. Moreover, a radical trapping experiment with TEMPO led to TEMPO-adduct **121** (Scheme 27b). These results suggest a single electron transfer from a Ni(I) or a Ni(II) species to the N–O bond. This single-electron transfer will form the iminyl radical **122** that could rapidly cyclize in a 5-*exo-trig* fashion to give the free carbon-centered radical **90** (Scheme 27c, path i). Nevertheless, these experiments did not rule out other pathways where the cyclization occurs in the coordination sphere of the metal after oxidative addition to a Ni(0) species. In this case, the C–N bond formation would go through the migratory insertion of the pendant alkene in the Ni–N bond. The carbon-centered radical intermediate **90** would result from the decoordination of the carbon ligand from the metal center (Scheme 27c, path ii).<sup>[101]</sup>

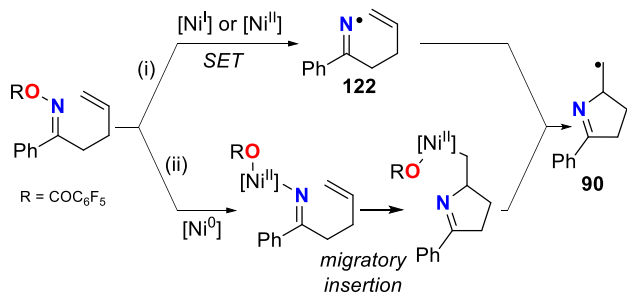
**a) 1,2-aminoarylation** (Selander et al., 2017)



**b) Experimental mechanistic investigation**



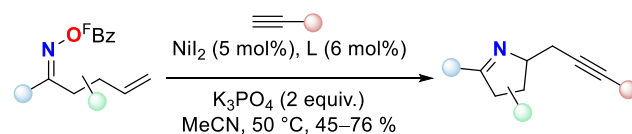
**c) Proposed mechanistic pathways towards a carbon-radical**



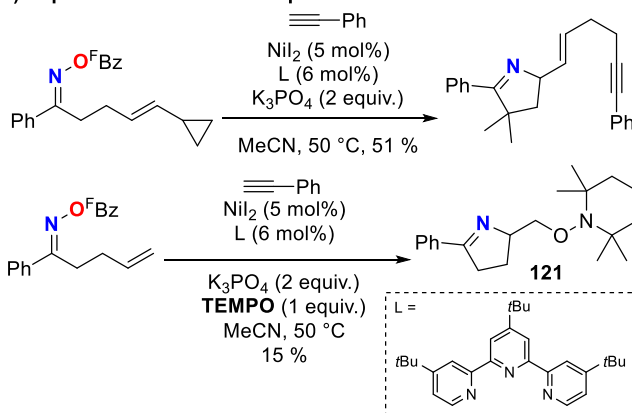
Scheme 27. a) 1,2-aminoarylation under Ni-catalysis involving a single-electron transfer as described by Selander et al.; b) Mechanistic investigations on the catalytic system; c) Proposed mechanistic pathways. TEMPO = (2,2,6,6-tetramethylpiperidin-1-yl)oxyl.

Recently, Zhang et al. reported a Ni-catalyzed iminoalkynylation based on a similar mechanistic rationale (Scheme 28a). Likewise, a radical clock experiment, where the pendant cyclopropyl underwent ring-opening, and a radical trapping experiment with TEMPO, which gave adduct **121** in 15% yield, hinted at a carbon-centered radical intermediate (Scheme 28b). Here again, these experiments cannot completely rule out a cyclization in the coordination sphere of the metal and give little information on the activation of the N–O bond itself.<sup>[102]</sup>

**a) Ni-catalyzed iminoalkynylation** (Zhang et al., 2021)



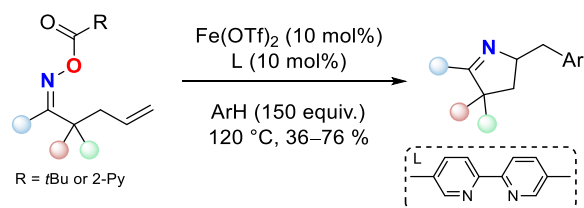
**b) Experimental mechanistic probes**



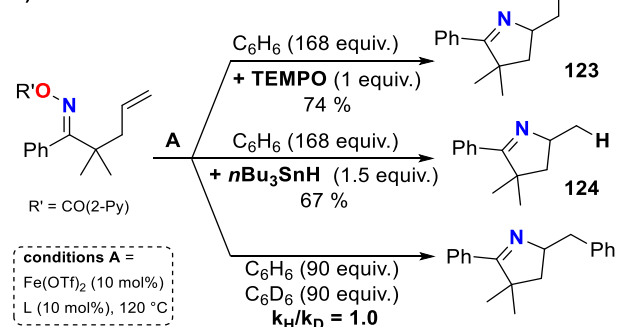
Scheme 28. a) Iminoalkynylation developed by Zhang et al. under Ni-catalysis; b) Mechanistic probes for this reaction.  $^{\text{F}}\text{Bz}$  = 3,5-bis(trifluoromethyl)benzoyl; TEMPO = (2,2,6,6-tetramethylpiperidin-1-yl)oxyl.

A similar iminoarylation was reported using Fe(II)-based catalysts by Ohe, Okamoto et al. (Scheme 29a). The authors proposed a carbon-centered radical intermediate. Indeed, only the TEMPO adduct **123** was detected in the presence of the radical scavenger TEMPO. Moreover,  $n\text{Bu}_3\text{SnH}$  completely suppressed the arylation, and only the hydrogenated product **124** was obtained. Finally, no kinetic isotopic effect was observed when using benzene- $\text{d}_6$  instead of benzene as the aryl partner (Scheme 29b).<sup>[103]</sup> The carbon-centered radical could also be trapped in a Giese-type reaction to synthesize tetrahydropyrrolizines.<sup>[104]</sup> The nature of the intermediate prior cyclization is yet unknown.

**a) Fe-catalyzed iminoarylation** (Ohe, Okamoto et al., 2018)



**b) Hints for a radical mechanism**



Scheme 29. a) Fe-catalyzed iminoarylation of oximes with a pendant alkene as disclosed by Ohe, Okamoto et al.; b) Mechanistic proofs for a radical pathway.

Radical mechanistic pathways thus occur mainly in reactions with oxime esters (or ethers) or phthalimide derivatives, which are

well-known electrophores. Seminal examples involved using stoichiometric amounts of metals and a 5-exo cyclization of a nitrogen radical on a pendant alkene. Apart from some examples, the following catalytic transformations include intramolecular reactions where a putative nitrogen radical cyclizes in a 5-exo-fashion. The resulting carbon radical was sometimes engaged in a cascade reaction allowing further functionalization of the 5-membered ring.

## 5. Conclusion

Since the seminal examples of reactions with hydroxylamine derivatives, many synthetic transformations have used the versatile reactivity of N–O  $\sigma$  bonds. Indeed, these weak bonds, which readily break in a homolytic fashion, are also easily reducible, undergoing single electron transfer from metallic species. Their radical reactivity accompanies an electrophilic reactivity, borne mainly by the nitrogen atom. More than making them react, the difficulty relies on obtaining the desired outcome. Combined with transition metal catalysis, the high reactivity of N–O bonds has already further improved on many classical methods, such as *N*-heterocycles syntheses, olefin amino-functionalization, or C–H amidation.

Few mechanistic investigations are reported compared to the large amounts of synthetic methodologies using N–O bond reactivity. Due to their high reactivity, isolating intermediate species is not always possible. Therefore mechanistic details of multiple transformations are not very clear. The borders between two different pathways are often faint, as exemplified by Bower et al. with the dichotomous reactivity of Pd-catalysts in the presence of oxime derivatives.<sup>[29]</sup> To investigate mechanistic features, characterization of intermediates through X-ray analysis when doable, radical-clock experiments to distinguish between polar and radical pathways (with careful attention to kinetics), or DFT computational studies are the most employed. One could also use kinetic studies, labeling experiments, and advanced spectroscopic analyses to identify the mechanisms at play. Although many transformations are reported, intermolecular reactions are rare in the case of oxidative additions or radical reactivity. Most reactions also lack atom economy since a sacrificial *O*-substituent (benzoate, electron-poor aromatic ring, pivalate...) is most of the time required. In only a few cases, the nitrogen and oxygen moieties are incorporated in the final molecule either through amino-oxygenation pathways with alkenes<sup>[73-74,92,105]</sup> or in alkylation reactions upon decarboxylation of the carboxylate moiety.<sup>[100]</sup> One can expect that understanding the critical features of the catalytic mechanistic pathways will offer more possibilities. Intermolecular reactions and the use of more available transition metals will be thus accessible. Moreover, employing both parts of the molecule more systematically will improve the atom economy of the transformations, like in the case of the photoexcited energy transfer reactions.<sup>[88]</sup> All the described methodologies thus set the stage for more challenging reactions.

## Acknowledgments

We acknowledge CEA, CNRS, the University Paris-Saclay, and ANR (project TransferNO, ANR JCJC Grant no. ANR-21-CE07-0060-01) for financial support.

**Keywords:** metal catalysis • N–O bonds • mechanisms • electrophilic amination • hydroxylamines

- [1] a) R. Hili, A. K. Yudin, *Nat. Chem. Biol.* **2006**, *2*, 284-287; b) A. Ricci, *Amino group chemistry: from synthesis to the life sciences*, John Wiley & Sons, **2008**; c) S. D. Roughley, A. M. Jordan, *J. Med. Chem.* **2011**, *54*, 3451-3479.
- [2] a) P. W. Neber, A. V. Friedolsheim, *Justus Liebigs Ann. Chem.* **1926**, *449*, 109-134; b) C. O'Brien, *Chem. Rev.* **2002**, *64*, 81-89.
- [3] E. Ciganek, in *Organic Reactions*, **2009**, p. 1-366.
- [4] K. S. Williamson, D. J. Michaelis, T. P. Yoon, *Chem. Rev.* **2014**, *114*, 8016-8036.
- [5] Y.-R. Luo, *Comprehensive Handbook of Chemical Bond Energies*, 1st edition ed., CRC Press, **2007**.
- [6] a) D. H. R. Barton, D. Crich, W. B. Motherwell, *J. Chem. Soc., Chem. Commun.* **1983**, 939-941; b) D. H. R. Barton, D. Crich, W. B. Motherwell, *Tetrahedron Lett.* **1983**, *24*, 4979-4982.
- [7] a) M. Hasebe, K. Kogawa, T. Tsuchiya, *Tetrahedron Lett.* **1984**, *25*, 3887-3890; b) M. Hasebe, T. Tsuchiya, *Tetrahedron Lett.* **1986**, *27*, 3239-3242.
- [8] a) J. A. Labinger, *Organometallics* **2015**, *34*, 4784-4795; b) The first report of an oxidative addition was described in the 1960s by reacting HCl with an Ir(I) complex: L. Vaska, J. W. Diluzio, *J. Am. Chem. Soc.* **1961**, *83*, 2784-2785.
- [9] A. J. Deeming, D. W. Owen, N. I. Powell, *J. Organomet. Chem.* **1990**, *398*, 299-310.
- [10] C. M. P. Ferreira, M. F. C. G. da Silva, V. Y. Kukushkin, J. J. R. F. da Silva, A. J. L. Pombeiro, *J. Chem. Soc., Dalton Trans.* **1998**, 325-326.
- [11] P. Arndt, C. Lefeber, R. Kempe, U. Rosenthal, *Chem. Ber.* **1996**, *129*, 207-211.
- [12] A. Tillack, P. Arndt, A. Spannenberg, R. Kempe, U. Rosenthal, *Zeit. Anorg. Allg. Chem.* **1998**, *624*, 737-740.
- [13] T. Shimbayashi, K. Okamoto, K. Ohe, *Chem. Eur. J.* **2017**, *23*, 16892-16897.
- [14] A. N. Desnoyer, W. Chiu, C. Cheung, B. O. Patrick, J. A. Love, *Chem. Commun.* **2017**, *53*, 12442-12445.
- [15] M. K. Bogdos, P. Muller, B. Morandi, *Organometallics* **2023**, *42*, 211-217.
- [16] H. Tsutsui, K. Narasaka, *Chem. Lett.* **1999**, *28*, 45-46.
- [17] a) For selected reviews on Narasaka group chemistry, see: M. Kitamura, K. Narasaka, *Chem. Record* **2002**, *2*, 268-277; b) K. Narasaka, *Pure Appl. Chem.*, **2003**, *75*, 19-28; c) K. Narasaka, M. Kitamura, *Eur. J. Org. Chem.* **2005**, *2005*, 4505-4519.
- [18] H. Tsutsui, M. Kitamura, K. Narasaka, *Bull. Chem. Soc. Jpn.* **2002**, *75*, 1451-1460.
- [19] a) M. Kitamura, S. Zaman, K. Narasaka, *Synlett* **2001**, *2001*, 974-976; b) S. Zaman, M. Kitamura, K. Narasaka, *Bull. Chem. Soc. Jpn.* **2003**, *76*, 1055-1062.
- [20] a) M. Kitamura, S. Chiba, O. Saku, K. Narasaka, *Chem. Lett.* **2002**, *31*, 606-607; b) S. Chiba, M. Kitamura, O. Saku, K. Narasaka, *Bull. Chem. Soc. Jpn.* **2004**, *77*, 785-796.
- [21] a) H. Tsutsui, K. Narasaka, *Chem. Lett.* **2001**, *30*, 526-527; b) C. A. Ramsden, M. Kitamura, D. Kudo, K. Narasaka, *Arkivoc* **2006**, *2006* (iii), 148-162.
- [22] S. Zaman, K. Mitsuru, A. D. Abell, *Org. Lett.* **2005**, *7*, 609-611.
- [23] M. Kitamura, Y. Moriyasu, T. Okauchi, *Synlett* **2011**, *2011*, 643-646.
- [24] T. Gerfaud, L. Neuville, J. Zhu, *Angew. Chem. Int. Ed.* **2009**, *48*, 572-577.
- [25] a) T. Nishimura, S. Uemura, *J. Am. Chem. Soc.* **2000**, *122*, 12049-12050; b) T. Nishimura, Y. Nishiguchi, Y. Maeda, S. Uemura, *J. Org. Chem.* **2004**, *69*, 5342-5347.
- [26] a) A. Furstner, K. Radkowski, H. Peters, *Angew. Chem. Int. Ed.* **2005**, *44*, 2777-2781; b) A. Furstner, K. Radkowski, H. Peters, G. Seidel, C. Wirtz, R. Mynott, C. W. Lehmann, *Chem. Eur. J.* **2007**, *13*, 1929-1945.

- [27] Y. Tan, J. F. Hartwig, *J. Am. Chem. Soc.* **2010**, *132*, 3676-3677.
- [28] W. P. Hong, A. V. Iosub, S. S. Stahl, *J. Am. Chem. Soc.* **2013**, *135*, 13664-13667.
- [29] N. J. Race, A. Faulkner, M. H. Shaw, J. F. Bower, *Chem. Sci.* **2016**, *7*, 1508-1513.
- [30] a) A. Faulkner, J. F. Bower, *Angew. Chem. Int. Ed.* **2012**, *51*, 1675-1679; b) A. Faulkner, J. S. Scott, J. F. Bower, *Chem. Commun.* **2013**, *49*, 1521-1523; c) N. J. Race, J. F. Bower, *Org. Lett.* **2013**, *15*, 4616-4619; d) A. Faulkner, J. S. Scott, J. F. Bower, *J. Am. Chem. Soc.* **2015**, *137*, 7224-7230; e) For a recent and detailed review on Narasaka-Heck type reactions work, see: N. J. Race, I. R. Hazelden, A. Faulkner, J. F. Bower, *Chem. Sci.* **2017**, *8*, 5248-5260.
- [31] X. Bao, Q. Wang, J. Zhu, *Angew. Chem. Int. Ed.* **2017**, *56*, 9577-9581.
- [32] C. Chen, L. Hou, M. Cheng, J. Su, X. Tong, *Angew. Chem. Int. Ed.* **2015**, *54*, 3092-3096.
- [33] I. R. Hazelden, X. Ma, T. Langer, J. F. Bower, *Angew. Chem. Int. Ed.* **2016**, *55*, 11198-11202.
- [34] a) I. R. Hazelden, R. C. Carmona, T. Langer, P. G. Pringle, J. F. Bower, *Angew. Chem. Int. Ed.* **2018**, *57*, 5124-5128; b) X. Ma, I. R. Hazelden, T. Langer, R. H. Munday, J. F. Bower, *J. Am. Chem. Soc.* **2019**, *141*, 3356-3360.
- [35] a) S. A. Shuler, G. Yin, S. B. Krause, C. M. Vesper, D. A. Watson, *J. Am. Chem. Soc.* **2016**, *138*, 13830-13833; b) R. D. Gao, S. A. Shuler, D. A. Watson, *Chem. Sci.* **2021**, *12*, 8859-8864.
- [36] F. Xu, S. A. Shuler, D. A. Watson, *Angew. Chem. Int. Ed.* **2018**, *57*, 12081-12085.
- [37] H. Tsutsui, Y. Hayashi, K. Narasaka, *Chem. Lett.* **1997**, *26*, 317-318.
- [38] S. Liu, Y. Yu, L. S. Liebeskind, *Org. Lett.* **2007**, *9*, 1947-1950.
- [39] Z. Zhang, Y. Yu, L. S. Liebeskind, *Org. Lett.* **2008**, *10*, 3005-3008.
- [40] a) A. M. Berman, J. S. Johnson, *J. Am. Chem. Soc.* **2004**, *126*, 5680-5681; b) A. M. Berman, J. S. Johnson, *J. Org. Chem.* **2005**, *70*, 364-366; c) A. M. Berman, J. S. Johnson, *J. Org. Chem.* **2006**, *71*, 219-224.
- [41] M. J. Campbell, J. S. Johnson, *Org. Lett.* **2007**, *9*, 1521-1524.
- [42] S. Tobisch, *Chem. Eur. J.* **2016**, *22*, 8290-8300.
- [43] Y. Miki, K. Hirano, T. Satoh, M. Miura, *Angew. Chem. Int. Ed.* **2013**, *52*, 10830-10834.
- [44] S. Zhu, N. Niljianskul, S. L. Buchwald, *J. Am. Chem. Soc.* **2013**, *135*, 15746-15749.
- [45] N. Guimond, S. I. Gorelsky, K. Fagnou, *J. Am. Chem. Soc.* **2011**, *133*, 6449-6457.
- [46] For an early example of nitrene formation starting with dioxazolones under thermo- and photolysis, see: J. Sauer, K. K. Mayer, *Tetrahedron Lett.* **1968**, *9*, 319-324.
- [47] G. Dequierez, V. Pons, P. Dauban, *Angew. Chem. Int. Ed.* **2012**, *51*, 7384-7395.
- [48] C. Wentrup, *Acc. Chem. Res.* **2011**, *44*, 393-404.
- [49] a) For one historical example of such reactivity, see: G. Smolinsky, B. I. Feuer, *J. Am. Chem. Soc.* **2002**, *86*, 3085-3088; b) for a comprehensive insight, see: M. M. Díaz-Requejo, A. Caballero, M. R. Fructos, P. J. Pérez, in *Alkane C-H Activation by Single-Site Metal Catalysis* (Ed.: P. J. Pérez), Springer Netherlands, Dordrecht, **2012**, p. 229-264; c) for an example where product selectivity is highly tuned, see: S. Y. Hong, Y. Park, Y. Hwang, Y. B. Kim, M. H. Baik, S. Chang, *Science* **2018**, *359*, 1016-1021.
- [50] Y. Ding, S. K. Sarkar, M. Nazish, S. Muhammed, D. Luert, P. N. Ruth, C. M. Legendre, R. Herbst-Irmer, P. Parameswaran, D. Stalke, Z. Yang, H. W. Roesky, *Angew. Chem. Int. Ed.* **2021**, *60*, 27206-27211.
- [51] a) P. F. Kuijpers, J. I. van der Vlugt, S. Schneider, B. de Bruin, *Chem. Eur. J.* **2017**, *23*, 13819-13829; b) For a review of electrophilic reactivity, see: P. Starkov, T. F. Jamison, I. Marek, *Chem. Eur. J.* **2015**, *21*, 5278-5300.
- [52] H. Noda, X. X. Tang, M. Shibasaki, *Helv. Chim. Acta* **2021**, *104*, e2100140.
- [53] K. Okamoto, T. Oda, S. Kohigashi, K. Ohe, *Angew. Chem. Int. Ed.* **2011**, *50*, 11470-11473.
- [54] H. J. Xie, F. R. Lin, L. Yang, X. S. Chen, X. C. Ye, X. Tian, Q. F. Lei, W. J. Fang, *J. Organomet. Chem.* **2013**, *745*, 417-422.
- [55] K. Okamoto, K. Sasakura, T. Shimbayashi, K. Ohe, *Chem. Lett.* **2016**, *45*, 988-990.
- [56] T. Shimbayashi, G. Matsushita, A. Nanya, A. Eguchi, K. Okamoto, K. Ohe, *ACS Catal.* **2018**, *8*, 7773-7780.
- [57] W. Rong, T. Zhang, T. Li, J. Li, *Org. Chem. Front.* **2021**, *8*, 1257-1266.
- [58] K. Okamoto, T. Shimbayashi, M. Yoshida, A. Nanya, K. Ohe, *Angew. Chem. Int. Ed.* **2016**, *55*, 7199-7202.
- [59] K. Okamoto, T. Shimbayashi, E. Tamura, K. Ohe, *Chem. Eur. J.* **2014**, *20*, 1490-1494.
- [60] T. Shimbayashi, K. Okamoto, K. Ohe, *Synlett* **2014**, *25*, 1916-1920.
- [61] C. L. Zhong, B. Y. Tang, P. Yin, Y. Chen, L. He, *J. Org. Chem.* **2012**, *77*, 4271-4277.
- [62] Y. Park, K. T. Park, J. G. Kim, S. Chang, *J. Am. Chem. Soc.* **2015**, *137*, 4534-4542.
- [63] P. W. Tan, A. M. Mak, M. B. Sullivan, D. J. Dixon, J. Seayad, *Angew. Chem. Int. Ed.* **2017**, *56*, 16550-16554.
- [64] K. S. Halskov, H. S. Roth, J. A. Ellman, *Angew. Chem. Int. Ed.* **2017**, *56*, 9183-9187.
- [65] R. H. Mei, J. Loup, L. Ackermann, *ACS Catal.* **2016**, *6*, 793-797.
- [66] J. Park, S. Chang, *Angew. Chem. Int. Ed.* **2015**, *54*, 14103-14107.
- [67] H. Lei, T. Rovis, *J. Am. Chem. Soc.* **2019**, *141*, 2268-2273.
- [68] G. N. Hermann, C. Bolm, *ACS Catal.* **2017**, *7*, 4592-4596.
- [69] V. Bizet, L. Buglioni, C. Bolm, *Angew. Chem. Int. Ed.* **2014**, *53*, 5639-5642.
- [70] X. Lyu, J. Zhang, D. Kim, S. Seo, S. Chang, *J. Am. Chem. Soc.* **2021**, *143*, 5867-5877.
- [71] S. Lee, T. Rovis, *ACS Catal.* **2021**, *11*, 8585-8590.
- [72] K. Okamoto, A. Nanya, A. Eguchi, K. Ohe, *Angew. Chem. Int. Ed.* **2018**, *57*, 1039-1043.
- [73] J. L. Jat, M. P. Paudyal, H. Gao, Q. L. Xu, M. Yousufuddin, D. Devarajan, D. H. Ess, L. Kurti, J. R. Falck, *Science* **2014**, *343*, 61-65.
- [74] D. F. Lu, C. L. Zhu, Z. X. Jia, H. Xu, *J. Am. Chem. Soc.* **2014**, *136*, 13186-13189.
- [75] a) For some examples, see: E. T. Hennessy, T. A. Betley, *Science* **2013**, *340*, 591-595; b) Y. Liu, X. Guan, E. L. Wong, P. Liu, J. S. Huang, C. M. Che, *J. Am. Chem. Soc.* **2013**, *135*, 7194-7204.
- [76] L. Legnani, B. Morandi, *Angew. Chem. Int. Ed.* **2016**, *55*, 2248-2251.
- [77] a) L. Legnani, G. Prina-Cerai, T. Delcaillau, S. Willems, B. Morandi, *Science* **2018**, *362*, 434-439; b) E. Falk, S. Makai, T. Delcaillau, L. Gurtler, B. Morandi, *Angew. Chem. Int. Ed.* **2020**, *59*, 21064-21071.
- [78] S. Makai, E. Falk, B. Morandi, *J. Am. Chem. Soc.* **2020**, *142*, 21548-21555.
- [79] a) H. Yu, Z. Li, C. Bolm, *Angew. Chem. Int. Ed.* **2018**, *57*, 324-327; b) S. Chatterjee, S. Makai, B. Morandi, *Angew. Chem. Int. Ed.* **2021**, *60*, 758-765.
- [80] S. Chatterjee, I. Harden, G. Bistoni, R. G. Castillo, S. Chhabra, M. van Gastel, A. Schnegg, E. Bill, J. A. Birrell, B. Morandi, F. Neese, S. DeBeer, *J. Am. Chem. Soc.* **2022**, *144*, 2637-2656.
- [81] Y. Zhou, J. Ni, Z. Lyu, Y. Li, T. Wang, G. J. Cheng, *ACS Catal.* **2023**, *13*, 1863-1874.
- [82] a) C. Chen, J. H. Zhao, X. N. Shi, L. Y. Liu, Y. P. Zhu, W. Sun, B. L. Zhu, *Org. Chem. Front.* **2020**, *7*, 1948-1969; b) J. C. Walton, *Molecules* **2016**, *21*, 63.
- [83] The use of phthalimide derivatives as redox-active esters has been recently reviewed: S. K. Parida, T. Manda, S. Das, S. K. Hota, S. De Sarkar, S. Murarka, *ACS Catal.* **2021**, *11*, 1640-1683.
- [84] K. Okada, K. Okamoto, M. Oda, *J. Am. Chem. Soc.* **1988**, *110*, 8736-8738.
- [85] a) For some selected examples, see: J. Boivin, A. C. Callier-Dublanchet, B. Quiclet-Sire, A. M. Schiano, S. Z. Zard, *Tetrahedron* **1995**, *51*, 6517-6528; b) K. Uchiyama, Y. Hayashi, K. Narasaka, *Chem. Lett.* **1998**, *27*, 1261-1262; c) F. Portela-Cubillo, J. S. Scott, J. C. Walton, *J. Org. Chem.* **2008**, *73*, 5558-5565; d) S. J. Markey, W. Lewis, C. J. Moody, *Org. Lett.* **2013**, *15*, 6306-6308; e) Y.

- Cai, A. Jalan, A. R. Kubosumi, S. L. Castle, *Org. Lett.* **2015**, *17*, 488-491.
- [86] a) For recent reviews, see: J. Davies, S. P. Morcillo, J. J. Douglas, D. Leonori, *Chem. Eur. J.* **2018**, *24*, 12154-12163; b) X. Y. Yu, Q. Q. Zhao, J. Chen, W. J. Xiao, J. R. Chen, *Acc. Chem. Res.* **2020**, *53*, 1066-1083; c) M. Latrache, N. Hoffmann, *Chem. Soc. Rev.* **2021**, *50*, 7418-7435; d) For selected examples on photoirradiation, see: R. Alonso, P. J. Campos, B. Garcia, M. A. Rodriguez, *Org. Lett.* **2006**, *8*, 3521-3523; e) F. Portela-Cubillo, E. M. Scanlan, J. S. Scott, J. C. Walton, *Chem. Commun.* **2008**, 4189-4191; f) R. T. McBurney, J. C. Walton, *J. Am. Chem. Soc.* **2013**, *135*, 7349-7354; g) M. Kitamura, Y. Mori, K. Narasaka, *Tetrahedron Lett.* **2005**, *46*, 2373-2376; h) M. Kitamura, K. Narasaka, *Bull. Chem. Soc. Jpn.* **2008**, *81*, 539-547; i) F. Gagosz, S. Z. Zard, *Synlett* **1999**, 1999, 1978-1980.
- [87] a) A. S. Mendkovich, M. A. Syroeshkin, D. V. Ranchina, M. N. Mikhailov, V. P. Gulyai, A. I. Rusakov, *J. Electroanal. Chem.* **2014**, *728*, 60-65; b) H. B. Zhao, P. Xu, J. Song, H. C. Xu, *Angew. Chem. Int. Ed.* **2018**, *57*, 15153-15156; c) X. Chang, Q. Zhang, C. Guo, *Org. Lett.* **2019**, *21*, 10-13; d) For a review, see: T. Wirtanen, E. Rodrigo, S. R. Waldvogel, *Adv. Synth. Cat.* **2020**, *362*, 2088-2101.
- [88] a) V. K. Soni, S. Lee, J. Kang, Y. K. Moon, H. S. Hwang, Y. You, E. J. Cho, *ACS Catal.* **2019**, *9*, 10454-10463; b) T. Patra, S. Mukherjee, J. Ma, F. Strieth-Kalthoff, F. Glorius, *Angew. Chem. Int. Ed.* **2019**, *58*, 10514-10520; c) T. Patra, P. Bellotti, F. Strieth-Kalthoff, F. Glorius, *Angew. Chem. Int. Ed.* **2020**, *59*, 3172-3177; d) For an account on N-O bond activation by energy transfer photocatalysis, see: D. S. Lee, V. K. Soni, E. J. Cho, *Acc. Chem. Res.* **2022**, *55*, 2526-2541.
- [89] a) C. Pratley, S. Fenner, J. A. Murphy, *Chem. Rev.* **2022**, *122*, 8181-8260; b) S. Z. Zard, *Chem. Soc. Rev.* **2008**, *37*, 1603-1618.
- [90] a) J. Boivin, A. M. Schiano, S. Z. Zard, *Tetrahedron Lett.* **1992**, *33*, 7849-7852; b) J. Boivin, A.-M. Schiano, S. Z. Zard, H. Zhang, *Tetrahedron Lett.* **1999**, *40*, 4531-4534.
- [91] F. Huang, S. Zhang, *Org. Lett.* **2019**, *21*, 7430-7434.
- [92] M. Noack, R. Gottlich, *Chem. Commun.* **2002**, 536-537.
- [93] Y. Koganemaru, M. Kitamura, K. Narasaka, *Chem. Lett.* **2002**, *31*, 784-785.
- [94] K. Tanaka, M. Kitamura, K. Narasaka, *Bull. Chem. Soc. Jpn.* **2005**, *78*, 1659-1664.
- [95] W. M. Liu, Z. H. Liu, W. W. Cheong, L. Y. T. Priscilla, Y. X. Li, K. Narasaka, *Bull. Korean Chem. Soc.* **2010**, *31*, 563-569.
- [96] M. N. Zhao, H. Liang, Z. H. Ren, Z. H. Guan, *Synthesis* **2012**, *44*, 1501-1506.
- [97] A. Faulkner, N. J. Race, J. S. Scott, J. F. Bower, *Chem. Sci.* **2014**, *5*, 2416-2421.
- [98] J. Ke, Y. Tang, H. Yi, Y. Li, Y. Cheng, C. Liu, A. Lei, *Angew. Chem. Int. Ed.* **2015**, *54*, 6604-6607.
- [99] L. Wang, C. Wang, *J. Org. Chem.* **2019**, *84*, 6547-6556.
- [100] W. Zhao, R. P. Wurz, J. C. Peters, G. C. Fu, *J. Am. Chem. Soc.* **2017**, *139*, 12153-12156.
- [101] H. B. Yang, S. R. Pathipati, N. Selander, *ACS Catal.* **2017**, *7*, 8441-8445.
- [102] X. J. Zhang, D. Qi, C. C. Jiao, Z. G. Zhang, X. P. Liu, G. S. Zhang, *Org. Chem. Front.* **2021**, *8*, 6522-6529.
- [103] T. Shimbayashi, K. Okamoto, K. Ohe, *Chem. Asian J.* **2018**, *13*, 395-399.
- [104] T. Shimbayashi, D. Nakamoto, K. Okamoto, K. Ohe, *Org. Lett.* **2018**, *20*, 3044-3048.
- [105] Such a reaction was reported with perfluorinated carboxylates under palladium catalysis: W. X. Wei, S. Chen, Y. Xia, M. Li, X. S. Li, Y. P. Han, C. T. Wang, Y. M. Liang, *ChemCatChem* **2019**, *11*, 5754-5757